

Thermal Analysis of a TREAT Fuel Assembly

Nuclear Engineering Division

About Argonne National Laboratory

Argonne is a U.S. Department of Energy laboratory managed by UChicago Argonne, LLC under contract DE-AC02-06CH11357. The Laboratory's main facility is outside Chicago, at 9700 South Cass Avenue, Argonne, Illinois 60439. For information about Argonne and its pioneering science and technology programs, see www.anl.gov.

DOCUMENT AVAILABILITY

Online Access: U.S. Department of Energy (DOE) reports produced after 1991 and a growing number of pre-1991 documents are available free via DOE's SciTech Connect (<http://www.osti.gov/scitech/>)

Reports not in digital format may be purchased by the public from the National Technical Information Service (NTIS):

U.S. Department of Commerce
National Technical Information Service
5301 Shawnee Rd
Alexandria, VA 22312
www.ntis.gov
Phone: (800) 553-NTIS (6847) or (703) 605-6000
Fax: (703) 605-6900
Email: orders@ntis.gov

Reports not in digital format are available to DOE and DOE contractors from the Office of Scientific and Technical Information (OSTI):

U.S. Department of Energy
Office of Scientific and Technical Information
P.O. Box 62
Oak Ridge, TN 37831-0062
www.osti.gov
Phone: (865) 576-8401
Fax: (865) 576-5728
Email: **reports@osti.gov**

Disclaimer

This report was prepared as an account of work sponsored by an agency of the United States Government. Neither the United States Government nor any agency thereof, nor UChicago Argonne, LLC, nor any of their employees or officers, makes any warranty, express or implied, or assumes any legal liability or responsibility for the accuracy, completeness, or usefulness of any information, apparatus, product, or process disclosed, or represents that its use would not infringe privately owned rights. Reference herein to any specific commercial product, process, or service by trade name, trademark, manufacturer, or otherwise, does not necessarily constitute or imply its endorsement, recommendation, or favoring by the United States Government or any agency thereof. The views and opinions of document authors expressed herein do not necessarily state or reflect those of the United States Government or any agency thereof, Argonne National Laboratory, or UChicago Argonne, LLC.

Thermal Analysis of a TREAT Fuel Assembly

prepared by
Dionissios Papadimas and Arthur E. Wright

Nuclear Engineering Division, Argonne National Laboratory

sponsored by
U. S. Department of Energy, National Nuclear Security Administration
Office of Material Management and Minimization

July 9, 2014

Table of Contents

1. Introduction	5
2. Thermal-hydraulic model of a single fuel assembly	6
2.1 Reference model and benchmarking with SINDA/G	6
2.2 Effect of pyrolytic graphite on cladding temperature.....	10
2.2.1 Sensitivity analysis – steady state (low power)	10
2.2.2 Sensitivity analysis – transient (high power)	12
3. Exploring options to reduce peak cladding temperatures	16
3.1 Fuel/cladding gap thickness and convective cooling.....	18
3.2 Replacing part of the fuel meat with pyrolytic graphite (PyGr).....	19
3.3 Effect of adding insulation between cladding and fuel meat	20
4. TREAT LEU design variants	24
4.1 TREAT LEU peak cladding temperatures	25
5. Summary and Conclusions	28
References	29
 Appendix I – Thermal Properties	31
 Appendix II – Peak fuel and cladding temperatures for scoping analysis	34
 Appendix III - Supporting information for TREAT LEU design variants	36
 Appendix IV. Effect of vacuum quality on peak cladding temperature	38

1. Introduction

The Transient Reactor Test Facility (TREAT) at Idaho National Laboratory is a large air-cooled test reactor fueled with highly enriched UO_2 dispersed in a graphite matrix. It can operate at steady state at nominally 100 kW power. The main purpose for which it was built, however, was to generate power transients. It was capable of producing a wide range of transients, with power levels in the hundreds of MW range for several seconds, or short power bursts reaching as high as 19 GW. Its core consists of a 19 x 19 array of 4-in x 4-in x 9-ft fuel and reflector assemblies, clad with 25 mil Zircaloy-3 around the fuel section and aluminum around the axial reflectors. The core is cooled with air forced axially downward through engineered channels between the assemblies. TREAT was constructed in the late 1950s and operated for almost 35 years. Since 1994, it has been in standby mode, but efforts are underway to prepare the facility for the resumption of transient testing later this decade.

This work was performed to support the feasibility study on the potential of TREAT core conversion from the use of fuel containing high-enriched uranium (HEU) to the use of fuel containing low-enriched uranium (LEU). An increase in the core energy is expected in order for the LEU core to deliver the same energy to a test sample as the HEU core. With an increase in peak fuel temperature, a critical issue in the TREAT fuel assembly design is to limit the cladding temperatures so as to preclude excessive cladding oxidation in the air atmosphere within the core.

The objective of this study was to explore options as to reduce peak cladding temperatures despite an increase in peak fuel temperatures. A 3D thermal-hydraulic model for a single TREAT fuel assembly was benchmarked to reproduce results obtained with previous thermal models developed for a TREAT HEU fuel assembly. In exercising this model, and variants thereof depending on the scope of analysis, various options were explored to reduce the peak cladding temperatures.

2. Thermal-hydraulic model of a single fuel assembly

2.1 Reference model and benchmarking with SINDA/G

The commercial software COMSOL® V 3.5a - a multiphysics platform based on the finite element method (FEM) - was used for the thermal analyses discussed in this work. The particular strength of the software is the capability to combine many physics interfaces (e.g. heat transfer, fluid flow, structural mechanics, corrosion, etc.) and thus extend the model beyond thermal-hydraulics if so needed.

Several models representing a single fuel assembly have been used depending on the scope of analysis in this work. A first important step in the analysis was to establish a reference model for evaluating limitations of simpler models previously used as well as to benchmark and reproduce the results obtained with previous thermal models developed for a TREAT fuel assembly [1,2]. The benchmark model for comparison was based on a three-dimensional thermal model of an HEU fuel assembly using the SINDA/G® code previously developed at ANL [1]. Computed fuel temperatures using that model were validated against measurements from old small-core experiments under steady-state operations (50 kW with cooling) as well as during a transient step response (445 MJ power pulse with 87 min. delayed cooling). Thus, for the reference model, the same geometry and assumptions as originally assumed using the SINDA/G® code will be used as summarized below.

Assuming negligible heat transfer between neighboring fuel assemblies, symmetry is utilized for the geometrical domain. Figure 1 shows a schematic of the fuel assembly and its cross section including some key dimensions of the nominal geometry. The benchmark model describes a 1/8th section of a single ~10-cm (4-in) square, 244-cm (8-ft) long fuel assembly within the TREAT reactor. Forced airflow on the outside of the cladding was originally modeled using independent flow channels indicated as “corner” and “side” flow as shown in Figure 1. The areas and hydraulic diameters of the respective flow sections were based on nominal dimensions and clearances. A mass-flow ratio¹ of ~9.4 to 1 between corner and side flow channels was estimated by assuming equal turbulent-flow pressure drops using the Blasius correlation [3,4]. Heat transfer coefficients between the forced air and cladding surfaces were calculated using the Dittus-Boelter correlation for the corner region and by an infinite parallel plate correlation for the side section respectively [3,5].

¹ Based on a nominal flow rate of 3250 cfm divided equally among 361 assemblies

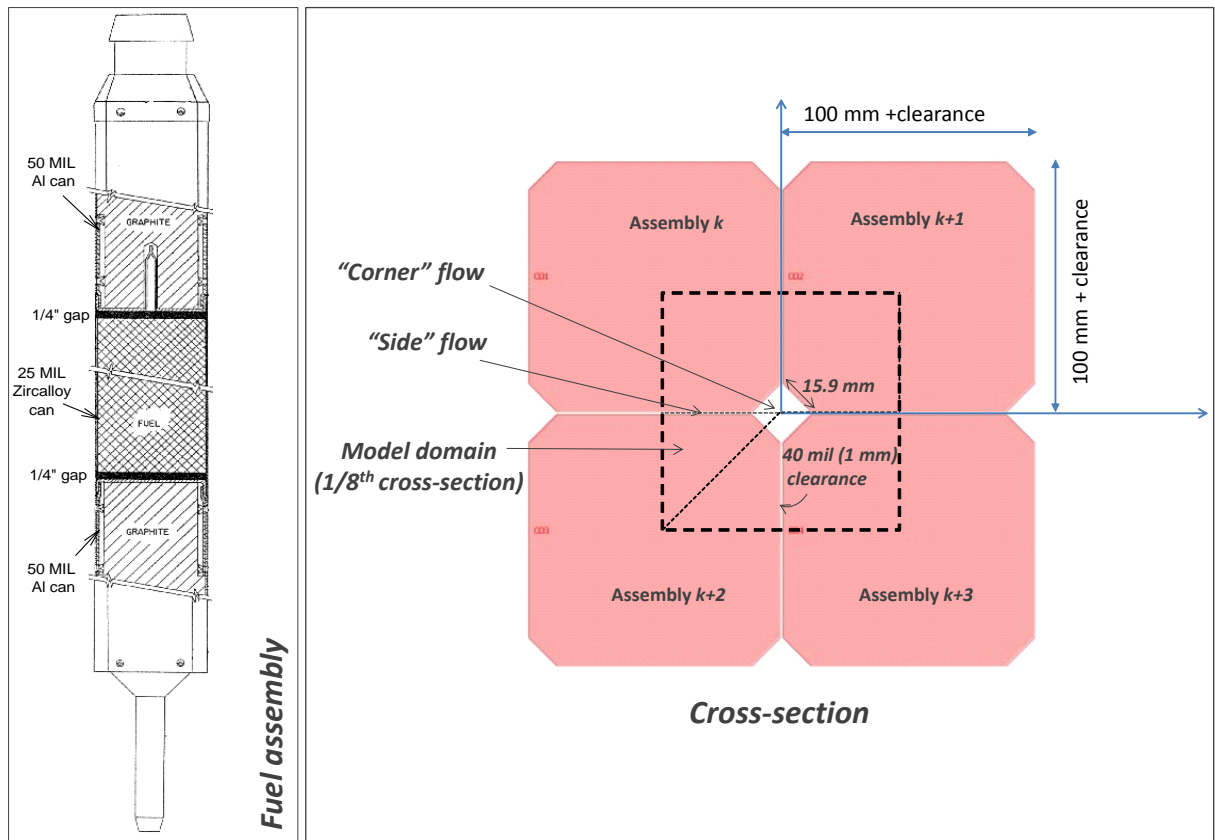


Figure 1. The model domain is represented by a 1/8th cross-section of a single TREAT fuel assembly.

The nominal geometry for the fuel assembly as implemented in the reference model is shown in Figure 2. The central section of the fuel assembly consists of a ~1.2-m long fuel block clad by 25 mils thickness of Zircaloy-3. Above and below the central section are two 0.6-m long blocks of aluminum-clad graphite reflector. By the use of Zircaloy spacers, the reflectors are separated from the fuel section by ~6-mm gaps.

Three dimensional conduction heat transfer is modeled within the fuel, reflector regions and cladding. Both thermal radiation and conduction is included in the gap between the fuel and reflectors as well as in the ~50 mil gap between fuel and Zircaloy cladding. Nominal thermal properties of materials used for the reference model are reported in Appendix I. As a conservative approach, it was assumed that a gas at reduced pressure is present in the gap between fuel and cladding wall with a conductivity equal to that of air at 1 atm. Effects such as distortions of the cladding wall, and possible points of direct contact with the fuel block, following evacuation of the air from inside the can have been ignored.

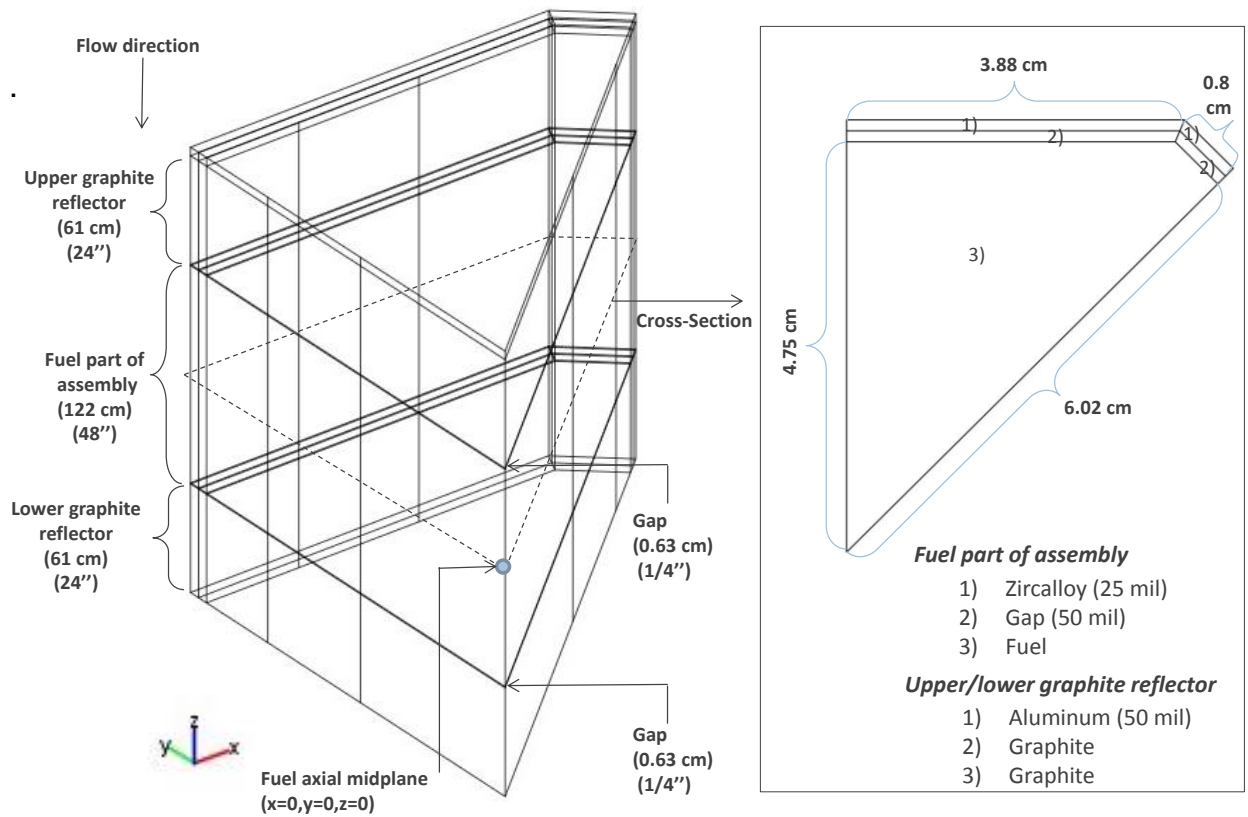


Figure 2. COMSOL® geometry and dimensions of a single TREAT fuel assembly. Reference thermal-hydraulic model.

Convective heat transfer for each flow channel (side and corner region) was coupled² to a one-dimensional energy balance for the respective region with heat-transfer correlations previously discussed. Air properties (viscosity, conductivity) are temperature dependent and evaluated from COMSOL's internal property libraries. The mesh used in the reference model consists of a total number of 70,000 nodes – representing a converged solution (no change in solution when using more nodes). A denser mesh is used in regions of sharp temperature profiles (e.g. at the fuel/reflector interfaces or near the wall boundaries). The energy balance of the flow was always verified and was 0.1% or less than the total energy input. In this report, unless otherwise mentioned, the term “gap” means a gap with a low quality vacuum such that both conductive and radiative heat transfer affect the overall heat transfer across the gap.

² Extrusion boundary and extrusion subdomain coupling variables were used in COMSOL to couple wall (3D model) and gas-phase temperatures for side and corner region (1D models). Twenty segments along the axial direction of the can (cladding) wall were used to calculate an average wall temperature along the periphery of the clad.

Figure 3 shows a representative comparison of temperature profiles between the reference model with results as calculated by SINDA/G [1]. This case shows steady-state temperature profiles for the fuel/reflector regions, cladding, and cooling air channels for a low-power steady-state operation at 50 kW and with 3250 cfm total air flow downward through the core (inlet temperature of 38 °C). A local axial peak to whole-core average power density of 1.7 was used for the calculations [1]. There is generally good agreement of calculated temperatures with the two different codes, this both for the wall temperatures as well as the axial temperature profile of the air-flow. The definition “side wall” and “corner wall” refer to specific coordinates in the x-y plane for which the temperature is evaluated, as indicated by the cross-section geometries. (In particular, “side wall” refers to the midpoint half way between the corners.) The side wall remains at a higher temperature relative to the corner region, a consequence of the disproportionally lower air-flow rate at the side section and hence low convective cooling. The fuel temperature (not shown) was almost in equilibrium with the side wall temperature (~ 10 °C difference).

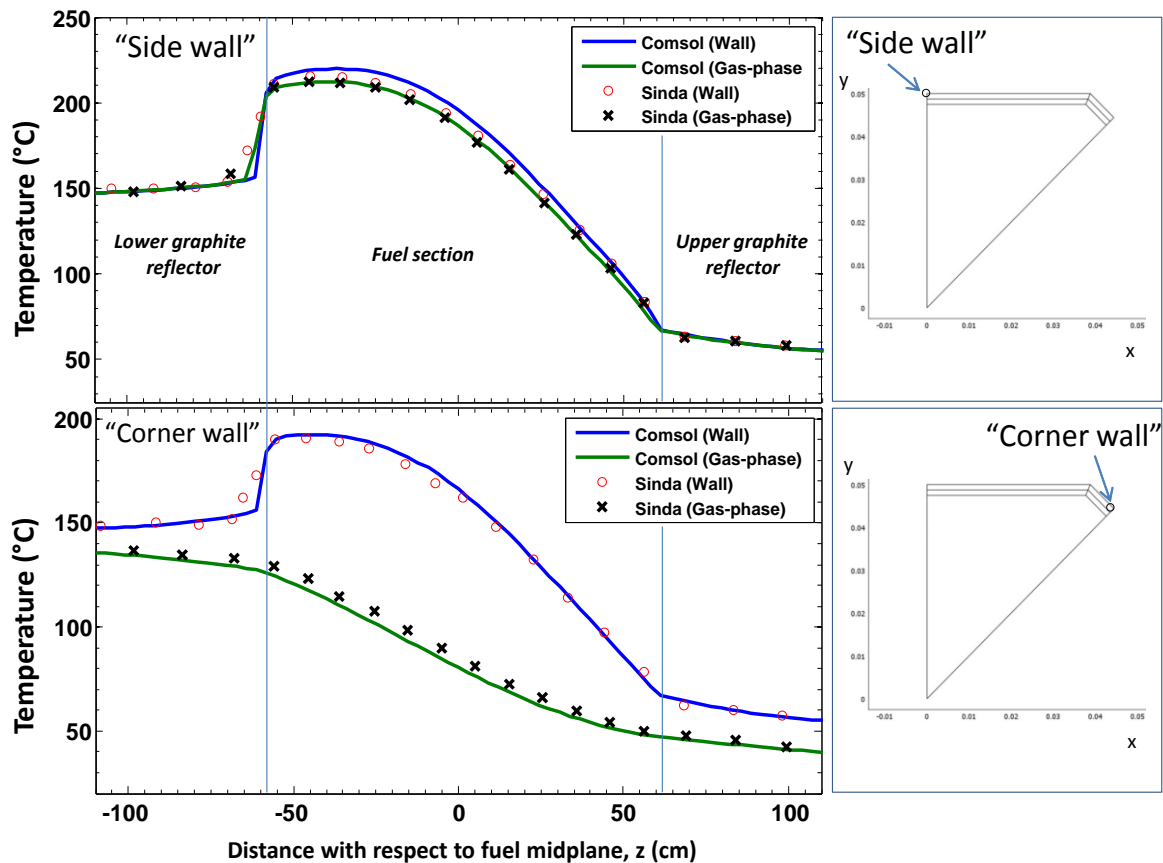


Figure 3. Comparison of COMSOL/SINDA results low-power steady-state operation at 50 kW.

2.2 Effect of pyrolytic graphite on cladding temperature

A question asked early on was whether the use of pyrolytic graphite (PyGr) replacing the gas gap could be used as a means to reduce the cladding temperature relative to the reference design of the fuel assembly (Figure 1). PyGr combine properties of low density and high in-plane thermal conductivity (up to 10 times higher than commercial graphite) and is extensively used as a means of effectively removing heat for instance in electronics [6]. Such substrates are highly anisotropic; the through-plane conductivity can be almost two orders of magnitude lower than the in-plane value, see Appendix I. Relative to graphite, the large difference in conductivity between the two planes of PyGr can reduce the heat transferred from the fuel to the cladding wall, yet allow the heat generated in the fuel to disperse axially and thus reduce peak axial cladding temperatures. Calculations using both COMSOL and SINDA/G were initially done in parallel which further served to compare/benchmark the results across the two different platforms. Both models predicted essentially similar temperature profiles (less than 10 °C variation), and for the most part COMSOL results will be shown in the discussion that follows below.

2.2.1 Sensitivity analysis – steady state (low power)

With a starting point of a low-power steady-state operation at 50 kW, the nominal 50 mil gap between fuel and Zircaloy cladding was filled either with graphite or pyrolytic graphite. Conductivity values as function of temperature for pyrolytic graphite are used as reported in Appendix I and are in good agreement with other sources in the literature (an in-plane to through-plane conductivity ratio of ~35).

Figure 4a shows steady-state axial temperature profiles along the cladding-wall section of the assembly when using graphite (Gr)/pyrolytic graphite (PyGr) in the 50 mil gap. Compared with the case of an empty gap (radiation heat transfer³) the temperature along the cladding-wall periphery, i.e. the wall section from side to the corner, is almost uniform when using Gr or PyGr. The peak wall temperature is also reduced when filling the gap with either graphite type (PyGr or normal graphite), especially at the side location of the cladding-wall. Using PyGr, however, with a high in-plane thermal conductivity the peak wall temperature is further reduced, a consequence of more heat being dispersed axially towards the upper graphite reflector.

Correspondingly, as shown in Figure 4b, the peak fuel temperature is reduced by ~ 60 °C when the gap between the fuel and Zircaloy inner wall is filled with PyGr.

³ Gas-phase conduction is also included in the calculations, but thermal radiation is the main heat transfer mode in the 50 mil gap. This topic is discussed in more detail in section 3.3.

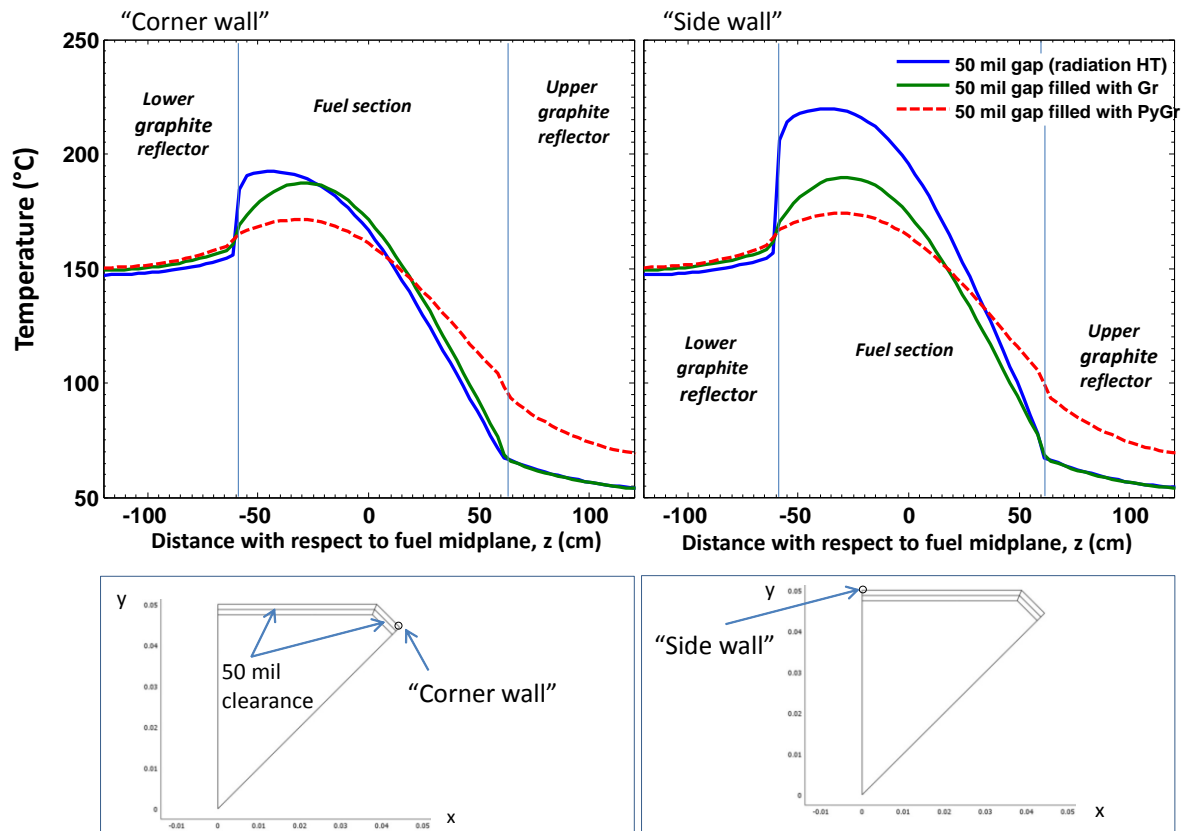


Figure 4a. Low-power steady-state operation at 50 kW, 3250 cfm air flow. Axial temperature gradients are reduced using graphite (Gr) or pyrolytic graphite (PyGr) in 50 mil gap.

Also shown in Figure 4b is a cross-section plot of the temperature profile from fuel center to corner outer wall. The cross-section displayed is evaluated at the fuel hot-spot (the axial location with the highest calculated temperature). Regardless whether the 50 mil gap is filled with graphite/pyrolytic graphite or not, cross-section temperature gradients within the fuel part of the assembly are very small.

Despite the relatively thin sheet of PyGr (50 mil) used, the above results indicate that the heat generated in the fuel could disperse axially and thus reduce peak axial cladding temperatures. However, the above case considered a rather limiting case considering a low power input at steady-state conditions. Further analysis was deemed necessary to evaluate the effectiveness of pyrolytic graphite to reduce the cladding temperature during power transients.

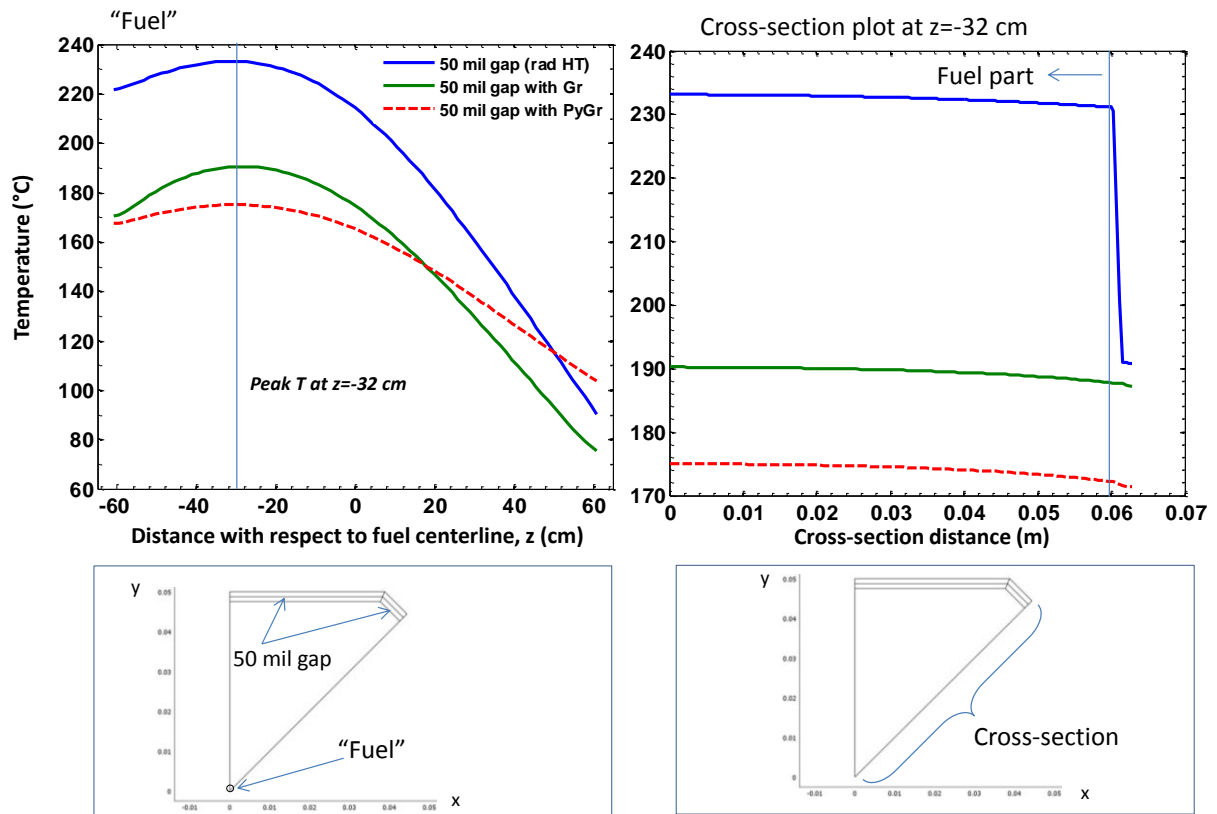


Figure 4b. Axial and cross-section temperature profile along fuel section of assembly.

2.2.2 Sensitivity analysis – transient (high power)

For the transient calculations, the core energy was deposited in a time-frame of 15 s leading to a total energy of 12.48 MJ per fuel assembly. The power time history was consistent with the original SINDA mode for comparison. Thermal properties and axial power profile for the hottest fuel assembly remain the same as used for the steady-state calculations discussed previously. The average power and consequently the temperature of the hottest fuel assembly reached 750 °C, a rather conservative value for any planned transient historically performed.

Figure 5 also shows the calculated axial temperature profile (50 mil gap) as function of time during a time interval of 20 s assuming no air flow. Proportional to the amount of energy input, the fuel temperature increases steeply between 5-15 s and gradually thereafter, reaching a peak fuel temperature of ~700°C 20 s after the power pulse was initiated. Both codes (SINDA and COMSOL) produced close to the same results for the transient cases.

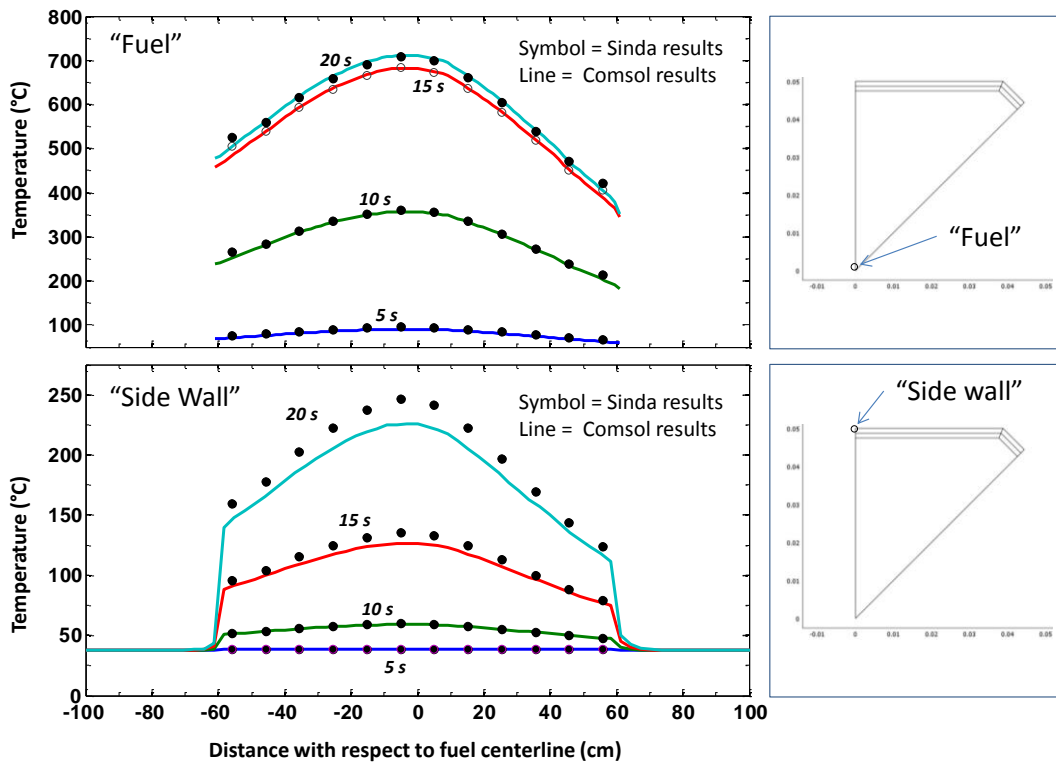


Figure 5. Axial fuel and cladding temperature profiles for the hottest assembly as a function of time.

The corresponding temperature profiles along the side section of the cladding wall are shown in Figure 6a. Here, the axial temperature profiles at select times are also shown for the additional cases when pyrolytic graphite (PyGr) is assumed to fill the 50-mil gap between the fuel and Zircaloy wall (50 mil clearance). PyGr affects the rate of change for cladding temperature. During the 20 s transient, the Zircaloy side wall temperature is rapidly heated for the cases when the gap contains PyGr as compared to the case with an empty gap (primarily thermal radiation as heat-transfer mode). The peak temperature of the cladding after 20 s for the latter case is still low at approximately 270 °C compared to 620 °C with a gap filled with PyGr. The maximum temperature of the cladding on the reflector is however still low, with a temperature of approximately 200 °C in both cases.

The calculations were repeated but with a coolant air-flow (3250 cfm, 38 °C) during the power transient to see if the air flow would affect the peak cladding temperature. There was almost no difference in the temperature profiles during the 20 s timeframe. Thus for this short duration, the coolant flow has a negligible impact on the temperature profiles relative to an adiabatic case.

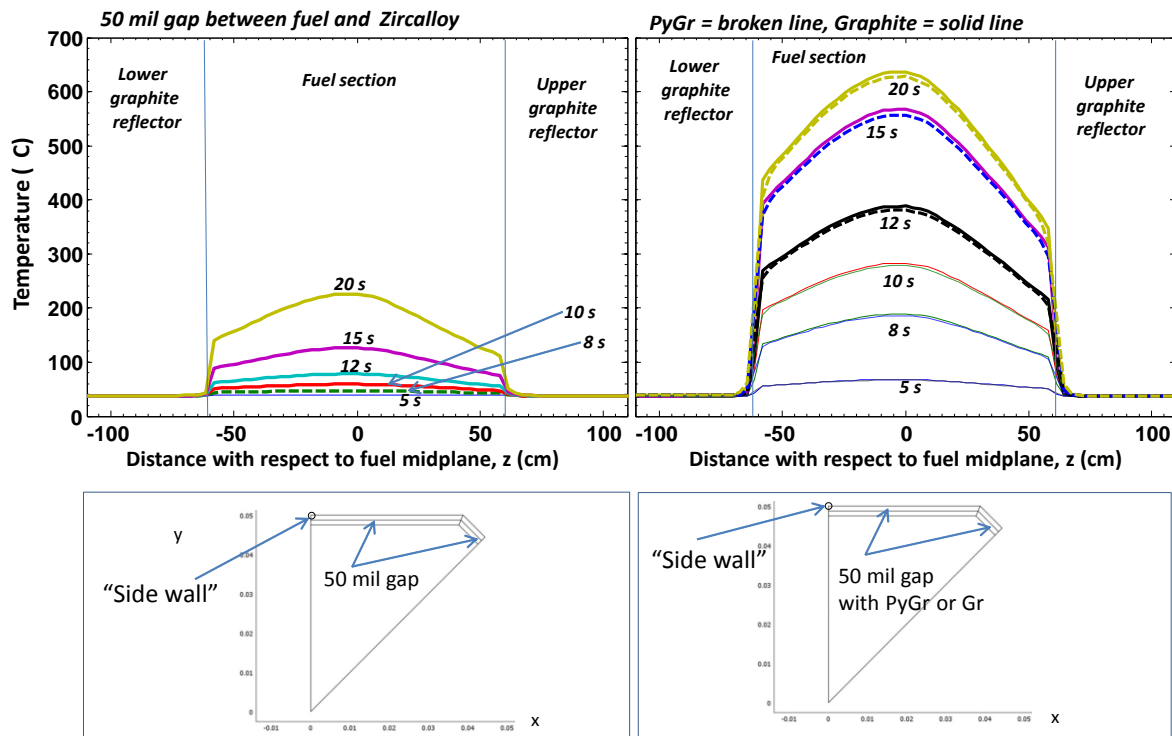


Figure 6a. The cladding in fuel section is rapidly heated when replacing the 50 mil empty gap with graphite (Gr) or pyrolytic graphite (PyGr).

The cladding temperature increase as a function of time shows a delay relative to the fuel temperature in the case of a 50 mil empty gap. However, in time, the temperature at the side region of the cladding wall will approach that of the fuel. Figure 6b shows the fuel and cladding temperature history under a longer timeframe after the power pulse was initiated. The temperature profiles are compared for the case with or without PyGr in the 50 mil gap at the fuel midplane ($z=0$). Regardless whether the gap is filled with PyGr, the fuel reaches a peak temperature of 750 °C after approximately 60 s and then gradually decreases due to convective cooling. In contrast with an empty gap, the fuel cools more rapidly with PyGr between the cladding and fuel a due to an additional thermal mass. After 100 s, the cladding reaches a peak temperature of ~700 °C, this for both scenarios calculated. The main difference between the cases is the temperature gradient along the cladding wall periphery (side to corner). Due to a low convective cooling in the side region, the side wall is significantly hotter than the corner region and in near equilibrium with the fuel temperature. PyGr is effective, however, to transfer the heat from the side to corner wall, although more of the cladding circumference reaches a higher temperature as a result.

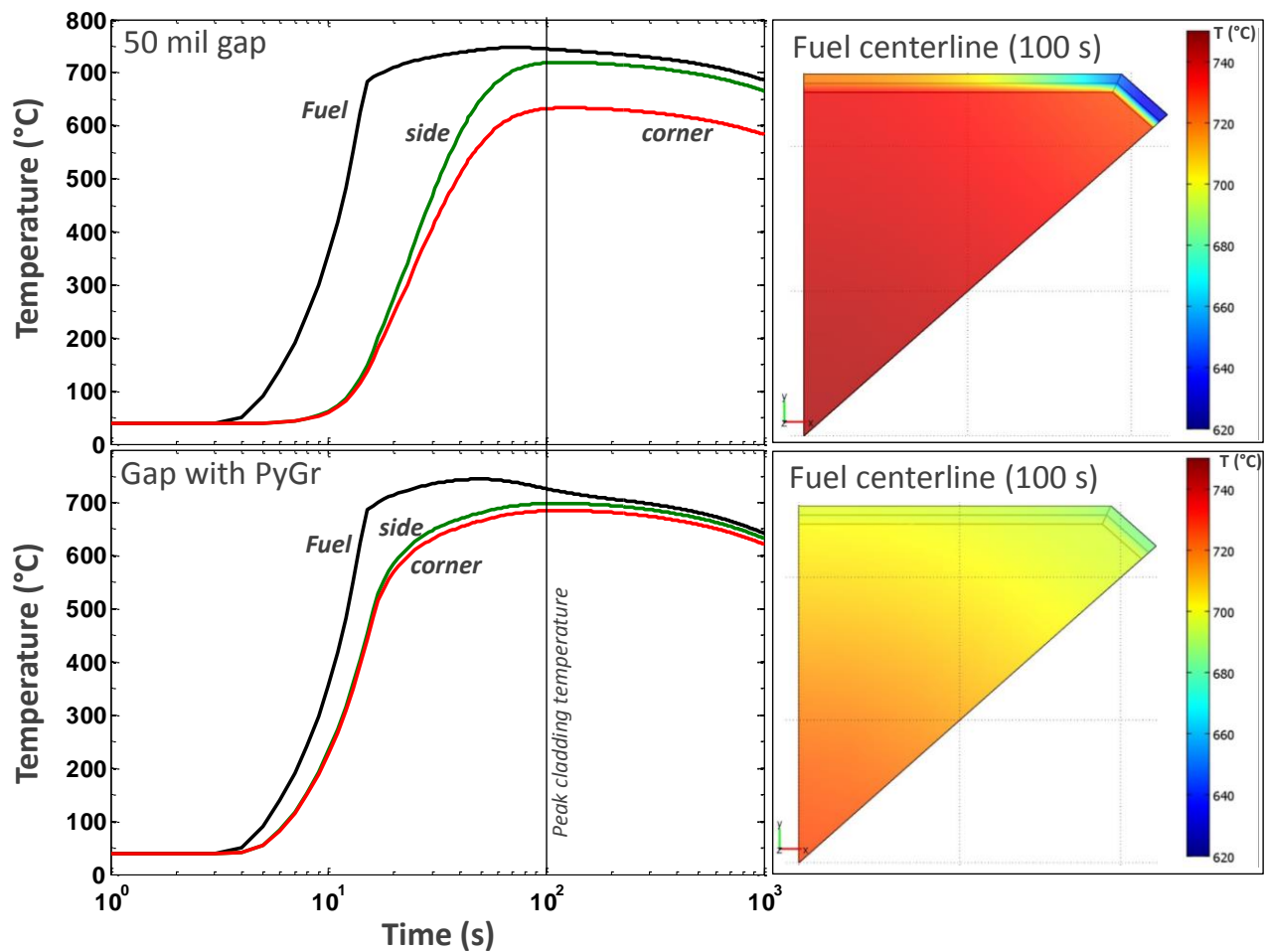


Figure 6b. *Pyrolytic graphite next to fuel and clad wall reduces temperature gradients but does not reduce the peak cladding temperature relative to an empty gap.*

While using PyGr results in almost uniform cross-sectional temperatures, it provides almost no benefit in reducing the peak cladding temperature relative to an empty gap. PyGr is not an insulator, and if in contact with fuel and wall, is only effective to minimize peripheral temperature gradients of the cladding (side-to-corner). Despite having high in-plane conductivity, the thin sheet of PyGr can by no means conduct the heat axially in a time scale of seconds.

3. Exploring options to reduce peak cladding temperatures

Initial calculations indicated that pyrolytic graphite may not be an effective strategy to reduce peak cladding temperatures, especially during a fast and high-energy power pulse. The initial analysis was limited in scope, however, and considered a thin sheet of PyGr in direct contact with the fuel meat and the cladding wall. PyGr by itself is not an effective insulator, but can be used to disperse heat depending on the time- and length-scales in focus.

Ideas were discussed of how to reduce the peak cladding temperatures, many of them merited further study. In the following discussion, some of the most pertinent scoping cases are reported on the effect of reducing peak cladding temperatures. The analysis considered the following cases.

- Increase the gap between the fuel and cladding wall to increase insulating effectiveness of both thermal radiation and gas-phase heat conduction as means of heat transfer in the gap.
- Replace a layer of fuel meat next to the gap by pyrolytic graphite to increase axial heat conduction. A nominal 50 mil gap between the cladding inner wall and graphite is maintained.
- Increase the air-flow rate and heat transfer between cladding wall and air to promote better cooling.
- Add insulating material between the cladding wall and fuel meat to increase insulating effectiveness.
- Keep the graphite reflector in intimate contact with the fuel to promote axial heat conduction.

Because of the many geometric and parametric changes required to address these cases, a simpler model was warranted to quickly estimate the peak cladding temperature for each case and variations within. The best cases could afterward be analyzed in more detail. The simplified model considers an axisymmetric geometry of the single fuel assembly [2]. The limitation of this model is that it estimates the temperature in the axial and radial direction and therefore resolves the peak cladding temperature only for the corner region. The temperature profiles as calculated with the axisymmetric model were compared to the 3D reference model (50 mil gap). All thermal properties, power profiles and power history were kept the same as discussed in section 2.2.2 but the average power⁴ of the fuel assembly was allowed to vary for sensitivity analysis. Figure 7 below shows an example of the fuel and cladding temperature profiles at the center of the fuel assembly as compared between the two models.

⁴ The average core energy of 1.96 GJ was assumed to be generated by 150-320 fueled assemblies

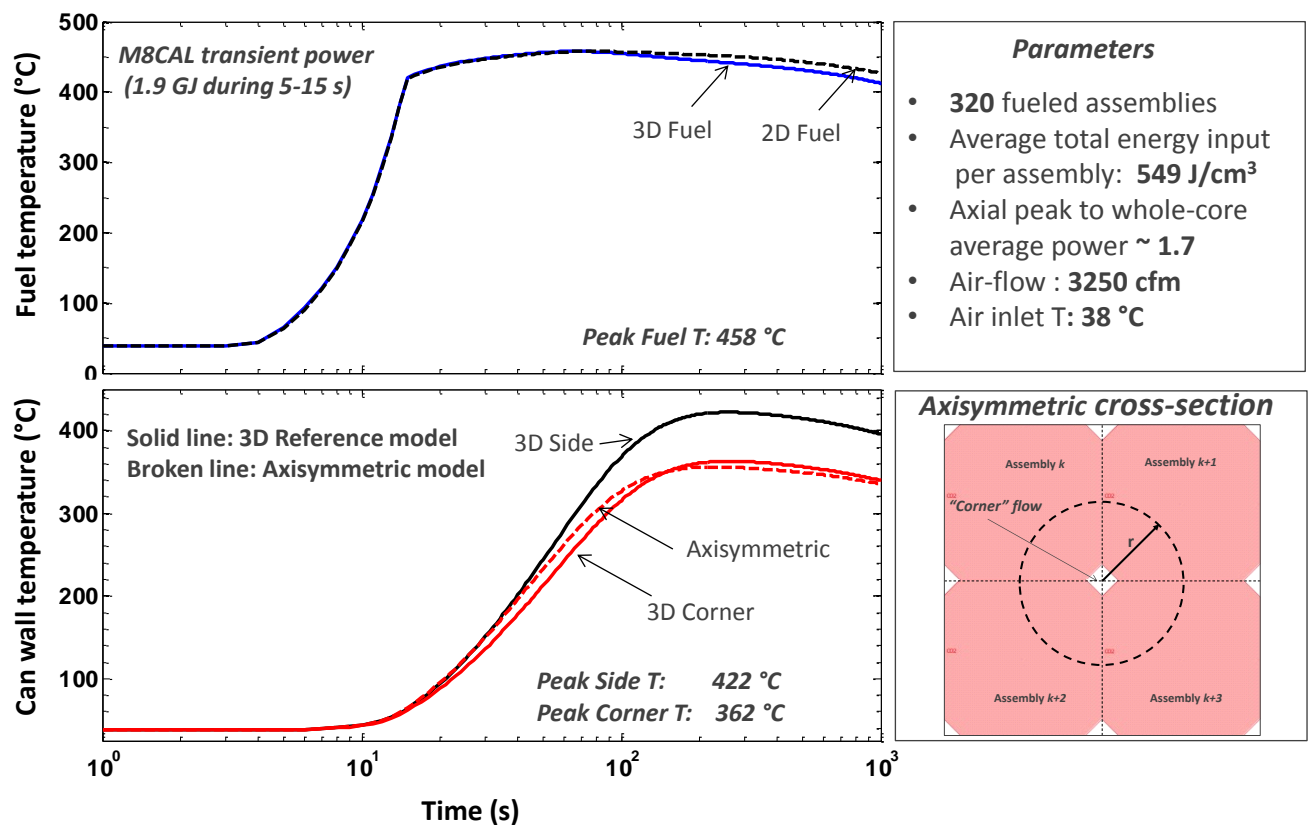


Figure 7. Results indicating the axisymmetric model is accurate enough for screening purposes; transient temperature profiles are in good agreement with the 3D model (fuel and "corner" wall)

For all cases, the axisymmetric model provided an accurate estimate of the peak fuel and cladding temperature (corner) as compared with the 3D reference model. The side and corner peak temperature calculated with the reference model showed progressively larger differences as the total energy per assembly increased (~ 100 °C as the peak fuel temperature exceeded 650 °C).

As a base/reference case for the following scoping analysis, the axisymmetric model used a total core energy of 12.48 MJ per fuel assembly (peak fuel temperature of 750 °C). Any variation from the reference case that may result in peak cladding corner temperatures below 500 °C would be considered for further analysis. A temperature well below 500 °C was conservatively estimated as to provide a large temperature margin and therefore ensure the side cladding temperature would be below 600 °C. Peak fuel and cladding temperatures for the reference case and all variants calculated are summarized in Appendix II. Key results for each case are discussed in the following sections.

3.1 Fuel/cladding gap thickness and convective cooling

The gap thickness between the fuel and cladding was systematically increased from a nominal thickness of 50 mil (base case) to $\sim \frac{1}{4}$ ". The outer dimensions of the fuel assembly remained the same, but the fuel thickness was reduced in 60-mil increments. Figure 8 below shows the peak fuel and peak cladding temperatures as functions of gap thickness and total air flow rate through the core. Doubling the flow rate did reduce the peak cladding temperature by approximately 100 °C but the thickness of the gap had a small effect on the temperature. Regardless of the air-flow rate, changing the empty gap thickness resulted in a modest decrease of the peak cladding temperature relative to the base case (~ 640 °C).

The reactor is cooled by an induced draft air system, and the cooling is controlled by two 40-hp turbo-compressors operating in parallel. Each turbo-compressor is rated at 3250 cfm [2]. For an air flow rate of 3250 cfm (one compressor), the temperature decreased by $\sim 20^{\circ}\text{C}$ as the gap thickness increased from 50 to 110 mil. Any further increase of the gap thickness slowly increased the peak cladding temperature, however. Since the total core energy remained fixed for all cases, any reduction in fuel volume increased the peak fuel temperature (because of the higher fuel power density) thus counteracting the corresponding insulating effect of increasing the gap thickness. By doubling the air flow-rate (6250 cfm), the peak cladding temperature decreased by $\sim 50^{\circ}\text{C}$ as the gap thickness increased from 50 to 170 mil and remained essentially constant with further increase in thickness.

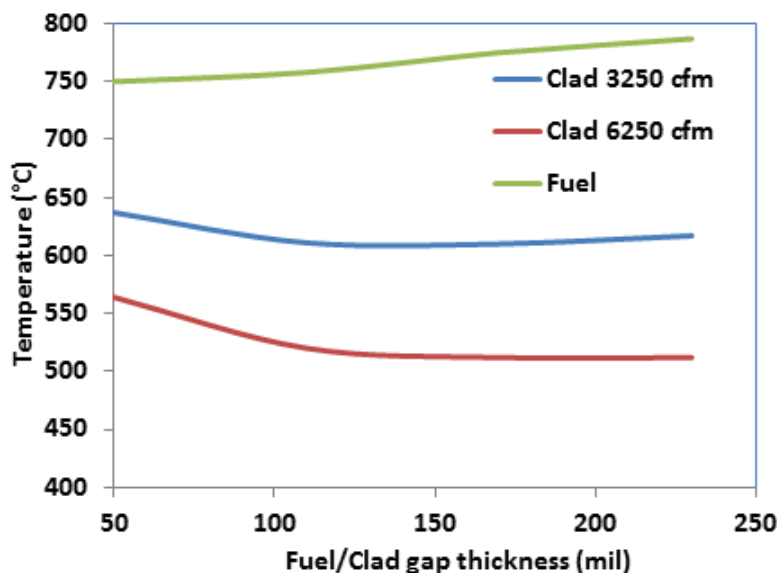


Figure 8. Peak fuel and peak cladding temperature as function of gap thickness and total air flow-rate.

The slight improvement is a consequence of the lower temperature of the cladding wall to begin with and corresponding reduction in gas-phase conductivity.

The weak effect of reducing the peak cladding temperature by increasing the gap thickness is perhaps not surprising. The overall heat transfer rate from fuel to cladding inner wall is controlled mainly by thermal radiation. Any increase in empty-gap thickness will reduce the heat conduction pathway but heat transfer by thermal radiation will remain virtually unchanged. Unless thermal radiation is impeded, increasing the gap thickness will have marginal benefits in reducing peak cladding temperatures. Increasing the air flow rate was a better option to reduce the cladding temperature at the corner region, but not enough to provide a large enough margin to warrant further side wall calculations. Increasing the heat-transfer rate to the coolant (e.g. surface roughness or surface area increase) may further reduce the cladding temperature as shown in Figure 9. Increasing the heat transfer rate by a factor of ~ 5 results in a decrease of the peak cladding temperature, but a further reduction⁵ is eventually limited by the total cooling capacity. If feasible, the combination of high air-flow rate and increase in heat-transfer rate may be useful in reducing the peak side cladding temperature.

3.2 Replacing part of the fuel meat with pyrolytic graphite (PyGr)

The effectiveness of PyGr to reduce cladding temperatures is next investigated with results shown below in Figure 10.

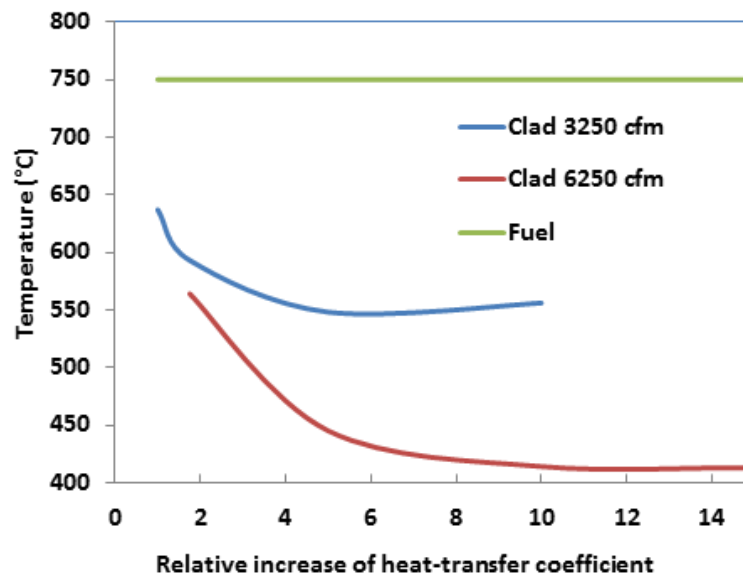


Figure 9. Results showing that a temperature difference between fuel and cladding of 300 °C is possible by greatly increasing the convective heat transfer rate and air flow-rate.

⁵ A slight increase in calculated cladding temperatures is observed when using high heat transfer rates. Due to a high convective heat transfer, the lower graphite reflector is heated from the gas-phase. This reduces the amount of heat that can be conducted from the fuel to the reflector.

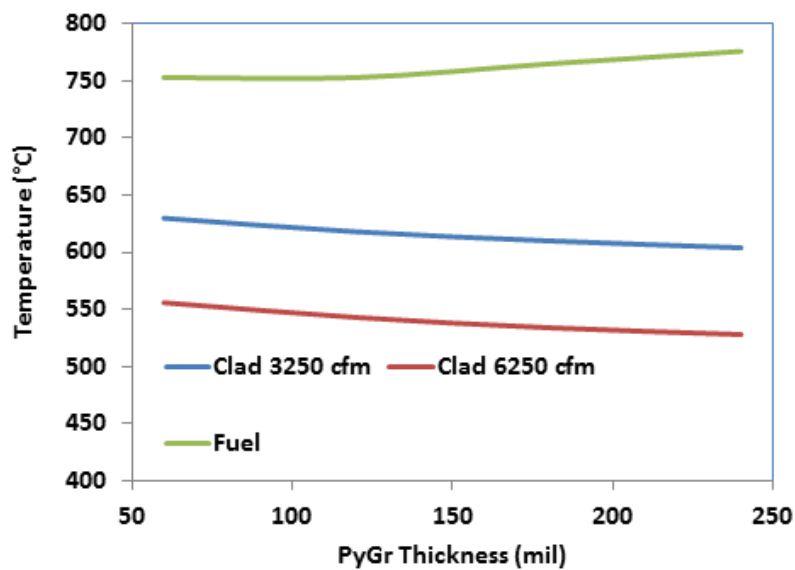


Figure 10. Results showing that placing the fuel meat with pyrolytic graphite is not an effective strategy to reduce axial peak cladding temperatures.

The fuel meat next to the cladding wall was incrementally replaced with 60 mils sheets of pyrolytic graphite. To avoid direct contact between the graphite and cladding, a nominal 50 mil empty gap was maintained between the inner cladding wall and the graphite surface. The usefulness of using PyGr as a means to disperse heat axially is marginal at best, even with large PyGr thicknesses. Even though a larger PyGr thickness tends to increase the axial heat flux, the effect is counteracted by an increasingly higher fuel temperature as the fuel volume is reduced. Increasing the gap by removing part of the fuel (see Figure 8) resulted in cooler cladding than did replacing the fuel volume with PyGr. This is because the temperature of the graphite remains at near equilibrium with the fuel, but the conduction pathway between cladding and PyGr remains constant at 50 mil.

3.3 Effect of adding insulation between cladding and fuel meat

Microporous insulation with operating temperatures as high as 950 °C was considered to be the reference material in the following calculations. Microporous insulation is more efficient at high temperatures than conventional insulation materials possessing excellent thermal conductivities, even better than still air. All thermal properties used for the calculations are reported in Appendix I. For all calculations, the insulation material was assumed to be in direct thermal contact with the fuel and inner wall of the cladding. The insulation thickness varied from 50-110-170 mil where the fuel meat was replaced by 60 mils or 120 mils of insulation material.

Figure 11 below shows the peak fuel and peak cladding temperatures as functions of insulation thickness and total air flow rate. Simply replacing the 50 mil empty gap with the insulating material significantly reduces the peak cladding temperature.

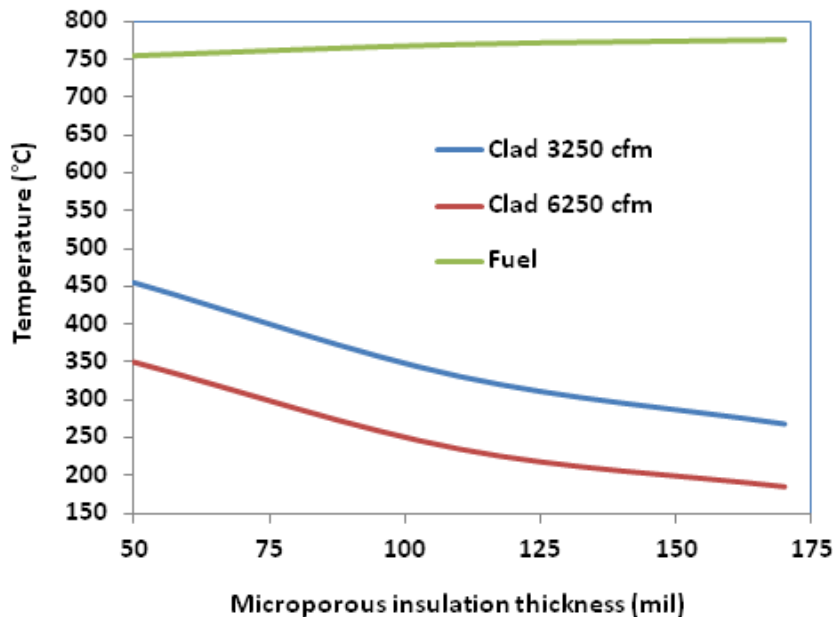


Figure 11. *Effect of microporous insulation thickness on peak cladding temperatures.*

For a flow rate of 3250 cfm, a 50 mil thick insulation reduced the peak cladding temperature by almost 200 °C relative to the base case (from 640 °C for an empty gap to ~450 °C). Increasing the insulation thickness reduced the peak cladding temperature further. For a thickness of 150 mil, the peak cladding temperature was below 300 °C, despite a continually increasing peak fuel temperature as the fuel volume was reduced. Increasing the air flow-rate to 6250 cfm reduced the peak cladding temperature by another 100 °C.

Some standard manufacturing dimensions and properties of microporous insulation, (i.e. thickness and chemical composition) may be of concern neutronically. The main composition of microporous insulation is SiO_2 with additions two or three compounds (depending on the manufacturer). Some insulating materials can contain over 10% TiO_2 , which will likely degrade neutronics due to the high thermal-neutron absorption cross-section of titanium. Some manufacturers also have a limit on the minimum insulation thickness during the manufacturing process, to ensure adequate mechanical strength of the material. Minimum

standard thicknesses, depending on vendor⁶, can range from less than 3 mm (120 mil) to over 6 mm (240 mil). Insulation that is too thick will result in a too-high axial neutron leakage.

A too-thick insulation is not desirable on a thermal-hydraulics basis because it significantly increases the cool-down time of the fuel assembly.

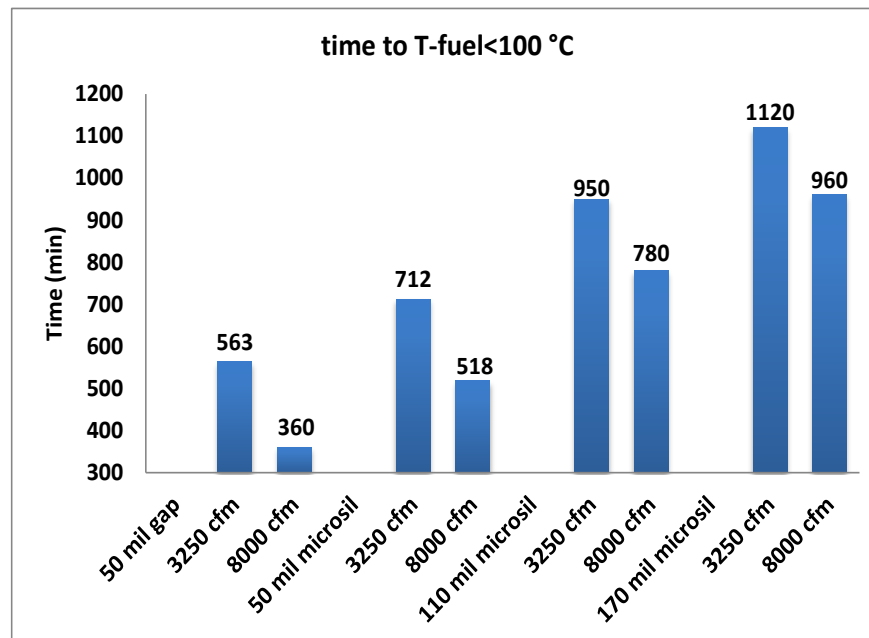


Figure 12. Cooling time as a function of air flow-rate and insulation thickness relative to the base case (50 mil empty gap).

Figure 12 shows the time required for the fuel to cool to below 100 °C after the power pulse was initiated (cooling from peak fuel temperatures of ~750 °C). For an air flow-rate of 3250 cfm, an estimated cooling of approximately 9 hours would be required for the base case (50 mil gap). With 50 mil thick microporous insulation, the cooling time increased to 12 hours and almost doubled relative to the base case for an insulation thickness of 170 mils to 19 hours. A reduction in cooling time, being more effective for thin insulations, was calculated if the air flow rate could be increased to 8000 cfm, provided such cooling capacity is available.

⁶ Microtherm® thin sheet microporous insulation for example is manufactured in a standard thickness of 3 mm. Thinner version may be available on request.

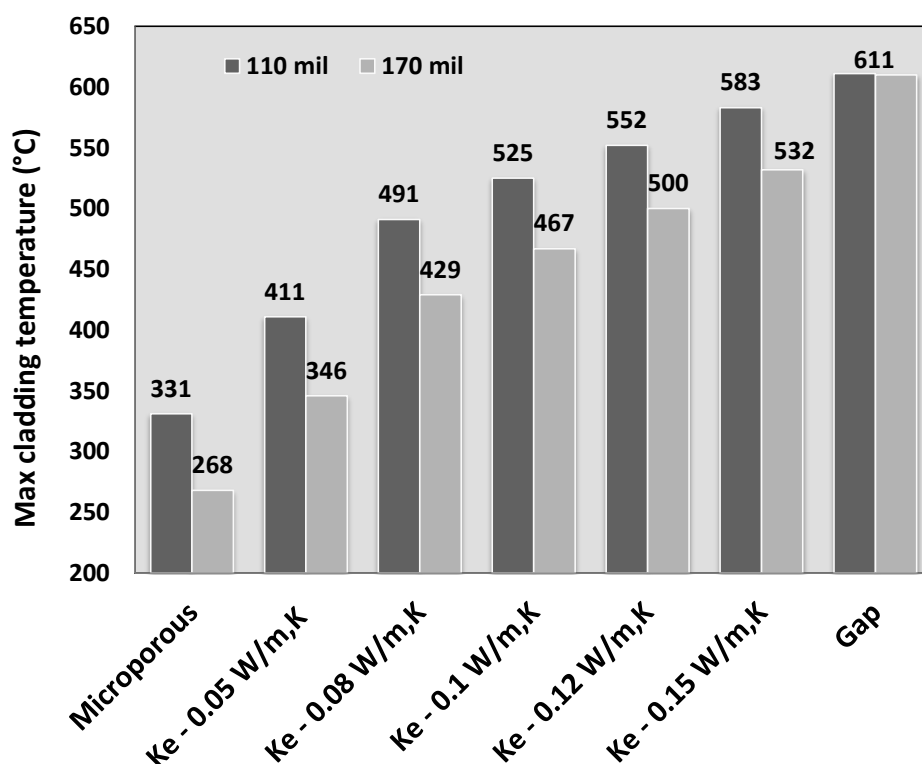


Figure 13. Effect of insulating effectiveness on peak cladding temperatures.

The effectiveness of insulating materials (or rather thermal properties) to reduce peak cladding temperature was also analyzed as shown below in Figure 13. The sensitivity analysis considered a range of effective conductivity values for the insulating material as long as the peak cladding temperature remained lower than the base case (50 mil empty gap). With a starting point of microporous insulation, the peak cladding temperature increased by about 100 °C for insulations with an effective conductivity (Ke) values equal to still air at 600 °C (0.06 W m⁻¹ K⁻¹). For an insulation thickness of 110 mil, a conductivity value of 0.15 W m⁻¹ K⁻¹ resulted in a cladding temperature almost as high as a 110 mil thick empty gap⁷. For such thickness, the conductivity of the respective insulating material must be 0.08 W m⁻¹ K⁻¹, preferably less, to ensure a peak side cladding temperature below 600 °C.

To ensure a side cladding temperature below 600 °C Insulations with a higher conductivity, up to 0.1 W m⁻¹ K⁻¹ may be acceptable by increasing the insulation thickness. With respect to insulation materials, microporous insulation with a thickness of less than 100 mil would be a preferable choice as a means of reducing peak cladding temperatures and allowing for an acceptable cooling time of the hottest fuel assembly.

⁷ While still air has a low conductivity, the clad temperature is higher relative to pure conduction due to thermal radiation from fuel to inner wall of the cladding.

4. TREAT LEU design variants

This section summarizes the thermal-hydraulics calculations for a set of TREAT LEU configuration options recommended by INL for neutronics and thermal-hydraulics analysis. The baseline option parameters, and variants thereof, are given in Table 1. For all cases, a single can (8 ft., 25 mils thick) of Zircaloy-3 is used for the cladding material, i.e. for both the fuel and reflector region. The reflector is also in direct contact with the fuel column. With exception of variants 1.3-1.6, an evacuated gap between the fuel and cladding with a nominal thickness of 50 mil is assumed. Variant 1.3 considers the effect of can wall deflection. Evacuation of the air from inside the can will likely cause distortion of large sections of the thin cladding wall.

Parameter	Baseline 1.0	Variant 1.1	Variant 1.2	Variant 1.3 ¹⁾	Variant 1.4	Variant 1.5	Variant 1.6
C/U ratio	1452	1452	1452	1452	1452	1452	1452
Boron	2.0	2.0	2.0	2.0	2.0	2.0	2.0
Fuel density (g/cm ³)	1.75	1.75	1.75	1.75	1.75	1.75	1.75
Fuel graphitization	70%	70%	85%	70%	70%	70%	70%
Core length (ft)	4	5	4	4	5	5	5
Insulation	none	none	none	None	none	1/16"	1/16"
PyG	none	none	none	None	1/8"	1/16"	1/16"

Table 1. TREAT LEU design base case and variants. Air cooling of 3000 cfm with an inlet temperature of 38 °C was assumed for all cases. ¹⁾43% of can side wall in direct contact with fuel. Var 1.5 has the insulation next to the cladding, and Var 1.6 has the insulation next to the fuel.

Based on structural analysis performed by INL, approximately 43% (in the horizontal direction) of the can side wall was in direct contact with the fuel under vacuum. Variants 1.4-1.6 consider replacing 1/16-in layers of the fuel meat next to the cladding with pyrolytic graphite (PyGr), or combinations of PyGr and microporous insulation (MP). For these cases, it was assumed that the cladding is in intimate contact with PyGr or MP along the fuel part of the assembly. Other variants include the amount of graphite content of the fuel, which primarily affects the thermal properties.

Neutronic calculations for all cases shown in Table 1 were done in parallel with results being the subject of a different report that is in preparation⁸. TREKIN-calculated power history was used as an input in the thermal-hydraulics calculations. Power history, axial power profiles for the hottest fuel assembly, and thermal properties used for this set of calculations are reported in Appendix III.

⁸ Personal communication with Dimitrios Kontogeorgakos, ANL, 2014.

4.1 TREAT LEU peak cladding temperatures

For the following calculations, the reference 3D model was adapted accordingly to estimate the peak cladding temperature along the periphery of the can wall (side to corner region, see Figure 2). The reflector was in direct contact with the fuel column. Sensitivity analysis showed that the peak cladding temperature was unaffected regardless if the reflector contacts the fuel column or if a ¼" gap is maintained as in the reference case. With exception of the fuel density and heat capacity, all other thermal properties remained the same as reported in Appendix I. The fuel heat capacity for 70% and 85% graphite content was approximated based on measured values for fuel block fabrication options under evaluation [7]. Values of thermal conductivity as a function of temperature measured for the various fuel blocks were close to the values reported in Appendix I. Core power history calculated with TREKIN for the LEU 4-ft core cases was used assuming an inserted reactivity that causes a peak fuel temperature of 600°C⁸.

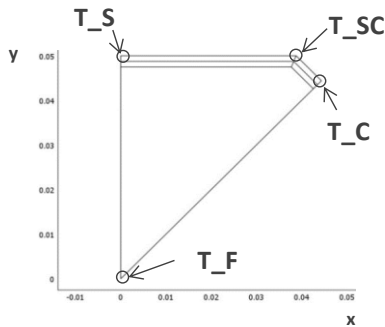
The effect of can wall deformation was modelled using an anisotropic gas-phase conductivity in the gap between cladding wall and fuel. The conductivity of the gap was set to zero (perfect vacuum) in the transverse direction as well as in the normal (perpendicular to the wall) direction where the can wall is not in contact with the wall. For the case where part of the side cladding wall contacts the fuel element (43%), a high conductivity was used to ensure thermal equilibrium between fuel/cladding. Variation of the cladding thickness due to deformation was neglected.

Table 2 below shows the calculated peak fuel and peak cladding temperatures for the base case and all variants as discussed previously. The peak temperatures are found near the maximum of the axial power profile and located within ~15 cm of the fuel centerline. The table highlights the peak cladding temperatures at three key locations along the can wall periphery: a) side region, b) intersection between side and corner wall and c) corner region.

For the baseline case (50 mil empty gap between the fuel and can wall), a peak fuel temperature as high as 643 °C is calculated⁹. The temperature of the corner region of the cladding wall is ~200 °C below the peak fuel temperature due to the convective cooling. In contrast, however, the side wall reaches a temperature as high as 600 °C; this is a

⁹ The calculated peak fuel temperature is higher than the anticipated value of 600 °C. The reason is that the fuel heat capacity values used for the 70% fuel graphite content are considerably lower than those used to generate the power profiles. Furthermore, an initial fuel temperature of 38°C was assumed for all cases considered.

Parameter	Baseline 1.0	Variant 1.0a	Variant 1.1	Variant 1.2	Variant 1.3	Variant 1.4	Variant 1.5	Variant 1.6
T_F (Fuel) (°C)	643	641	556	605	627	613	595	604
T_S (°C)	603	626	508	562	622	549	498	393
T_SC (°C)	488	544	400	450	497	545	405	389
T_C (°C)	457	518	373	420	465	544	384	388



Definitions

T_F : Peak Fuel temperature

T_S: Peak cladding temperature (far Side region)

T_SC: Peak cladding temperature (Side/Corner intersection)

T_C: Peak cladding temperature (Corner region)

Table 2. Calculated peak fuel and peak cladding temperatures for TREAT LEU design base case and variants.

- Baseline 1.0: 4 ft. core, 50 mil empty gap
- Variant 1.0a: 4 ft. core, 50 mil gas-filled gap at atmospheric pressure
- Variant 1.1: 5 ft. core, 50 mil empty gap
- Variant 1.2: 4 ft. core, 50 mil empty gap, 85% fuel graphitization
- Variant 1.3: 4 ft. core, empty gap but side cladding wall in partial contact with fuel
- Variant 1.4: 5 ft. core, 1/8" PyGr replaces fuel meat
- Variant 1.5: 5 ft. core, 1/16" MP next to cladding, 1/16" PyGr next to fuel
- Variant 1.6: 5 ft. core, 1/16" PyGr next to cladding, 1/16" MP next to fuel

PyGr = pyrolytic graphite

MP = Microporous insulation

All cases, except variant 1.2 assume 70% fuel graphitization

consequence of almost stagnant flow conditions in this region and the small amount of heat that can be conducted to the corner region due to the small thickness of the cladding wall.

In contrast, the calculated temperatures for variant 1.2 were ~ 40 °C lower for both the fuel and side can wall region. The reason is the different graphite content of the fuel and consequently the differences in fuel heat capacity values used for these two cases.

Variant 1.0a (added to the INL set) considers, in addition to thermal radiation, the effect of gas-phase conductivity in the 50 mil gap. If the gap is not completely evacuated, or if a gas is present at low pressures, gas-phase heat conduction becomes important. At ~ 1 mbar the conductivity of the gas approaches the corresponding value at atmospheric pressure; see Appendix IV for supporting calculations. The increase in temperature when the gap is not completely evacuated is more pronounced at the corner section (60 °C difference) vs ~ 20 °C as calculated in the side wall relative to the base case. In any event, if the can wall cannot be maintained at a low enough pressure, or if the side cladding wall contacts the fuel element, variant 1.3, the side wall of the cladding will be in near equilibrium with the fuel temperature.

Notwithstanding the effect on neutronics, for the same core power, longer fuel results in lower fuel and cladding temperatures. The peak fuel and peak side can wall temperature for Variant 1.1 (5 ft. core) is reduced by almost 100 °C relative to the base case. Based on previous results, using PyGr to reduce peak cladding temperature is likely to have a small effect. Adding a 1/8" thick layer of pyrolytic graphite (Variant 1.4), however, resulted in even higher temperatures relative to Variant 1.1, this both for the fuel and along the can periphery. For constant core power and replacing part of the fuel meat with PyGr, resulted in almost 60 °C higher fuel temperatures. The can wall remained at a high and almost uniform temperature from the side to the corner region of the cladding wall.

Adding 1/16" of microporous insulation (MP) next to the cladding followed by 1/16" of PyGr next to the fuel meat (Variant 1.5) did not result in a significant improvement relative to Variant 1.1¹⁰. The insulating capacity of MP resulted in slightly lower temperatures for the side region of the can wall, despite a higher fuel temperature. PyGr next to the fuel meat had little effect on reducing temperature gradients axially, and fuel cross-section temperature gradients are small to begin with. In this case, replacing part of the fuel meat with PyGr had the effect of increasing the fuel temperature instead. A better option from a thermal-hydraulics standpoint would be to use a 1/16" thick MP insulation only.

¹⁰ *This assumes an idealized scenario that the side can wall will not contact the fuel upon evacuation. Unless the cladding thickness is increased, a 25 mil cladding will contact the fuel and be in thermal equilibrium with the fuel.*

Variant 1.6 considered the case of reversing the location of MP/PyGr (MP next to the fuel) and shows the most encouraging results to reduce peak cladding temperatures. MP insulation reduces the heat flux from the fuel to the graphite and also allows the graphite to redistribute the heat evenly along the periphery of the cladding wall (side to corner region). The temperature is uniform along the entire cladding wall, and the peak wall temperature is more than 100 °C lower than in variant 1.1 (side wall). If account were taken that the side cladding may contact the fuel following an evacuation of the gap (a 5-ft core version of variant 1.3), the effect would be considerably larger.

5. Summary and Conclusions

A 3D thermal-hydraulic model for a single TREAT fuel assembly was benchmarked to reproduce results with previous thermal models developed for a TREAT HEU fuel assembly. Exercising this model, and variants thereof depending on the scope of analysis, explored options as to reduce the peak cladding temperature relative to the HEU fuel basic design.

- Compared to a 50-mil empty gap between fuel and cladding, adding a layer of pyrolytic graphite inside the gap provides no benefit to reduce the peak cladding temperature during a transient. Maintaining a 50 mil empty gap and replacing the fuel meat with varying thicknesses of pyrolytic graphite provided little benefit in reducing the cladding temperature for the same fuel assembly total power. The pyrolytic graphite is effective to reduce the thermal gradients along the periphery of the cladding wall but it is not an insulator. Increasing the gap from 50 mils to 250 mils also makes little change in the peak cladding temperature.
- The peak cladding temperature, even during a transient, is greatly affected by the rate of air flow at the assembly corners. Reducing the temperatures along the side of the cladding wall represents the biggest challenge, however. Given a low convective cooling and thin cladding, the amount of heat that can be transferred along the side wall to the corner region is limited. Evacuating the gap (perfect vacuum) between the fuel and cladding helps to reduce peak cladding temperature with a margin relative to the peak fuel temperature of ~50°C. However, potential methods of stiffening the can wall would be necessary to avoid direct contact with the fuel.
- High (standard) density insulator between fuel and cladding may not substantially reduce the peak cladding temperature relative to a 50 mil empty gap. The thermal conductivity will be too high to significantly reduce the peak cladding temperature. Microporous insulation with a thermal conductivity lower than stagnant air is more effective in limiting peak cladding temperature than an empty gap of the same thickness. Adding both a thin sheet of microporous insulation next to the fuel and a

sheet of PyGr next to the cladding wall reduces peak cladding temperatures well below peak fuel temperature and also reduces thermal gradients along the periphery of the cladding wall.

References

- [1] Bauer, T., Argonne National Laboratory, unpublished information, 2014.
- [2] Freund, G.A., Elias, P., MacFarlane, D.R., Geier, J.D., 1960. Design Summary Report on the Transient Reactor Test Facility (TREAT). Argonne National Laboratory. ANL-6034, p. 130.
- [3] Bird, R.B., Stewart, W.E., Lightfoot, E.N., 1960. Transport Phenomena. John Wiley & Sons, New York.
- [4] McKeon, B.J., Zagarola, M.V., Smits, A.J., 2005. A new friction factor relationship for fully developed pipe flow. *Journal of Fluid Mechanics* 538, 429-443.
- [5] Kays, W.M., Crawford, M.E., 1993. Convective Heat and Mass Transfer. McGraw-Hill, New York.
- [6] Heusch, C.A., Moser, H.G., Kholodenko, A., 2002. Direct measurements of the thermal conductivity of various pyrolytic graphite samples (PG, TPG) used as thermal dissipation agents in detector applications. *Nuclear Instruments and Methods in Physics Research A* 480, 463-469.
- [7] Lessing, P.A., 2014. Test Results for Characterization of TREAT Fuel Fabricated Using Extrusion and Overcoat-Compacting Methods. Idaho National Laboratory. p. 38.
- [8] Incropera, F.P., DeWitt, D.P., 1985. *Introduction to Heat Transfer*. John Wiley & Sons, New York.
- [9] Sheppard, R.G., Mathes, D.M., Bray, D.J., 1987. Properties and Characteristics of Graphite, Poco Graphite, Inc. p. 50.
- [10] Ainscough, J.B., 1982. Gap Conductance in Zircaloy-Clad LWR Fuel Rods. Committee on the Safety of Nuclear Installations OECD Nuclear Energy Agency. CSNI Report No. 72, p. 57.
- [11] International_Atomic_Energy_Agency, 2006. Thermophysical properties database of materials for light water reactors and heavy water reactors. IAEA-TECDOC-1496, p. 404.
- [12] Murabayashi, M., Tanaka, S., Tkahashi, Y., 1975. Thermal Conductivity and Heat Capacity of Zircaloy-2, -4 and Unalloyed Zirconium. *Journal of Nuclear Science and Technology* 12, 661-662.

- [13] Beikircher, T., Goldmund, G., Benz, N., 1996. Gas Heat Conduction in an Evacuated Tube Solar Collector. *Solar Energy*, 58, 213-217.
- [14] Redhead, P.A., 1968. *The Physical Basis of Ultra-High Vacuum*. Chapman & Hall, London.

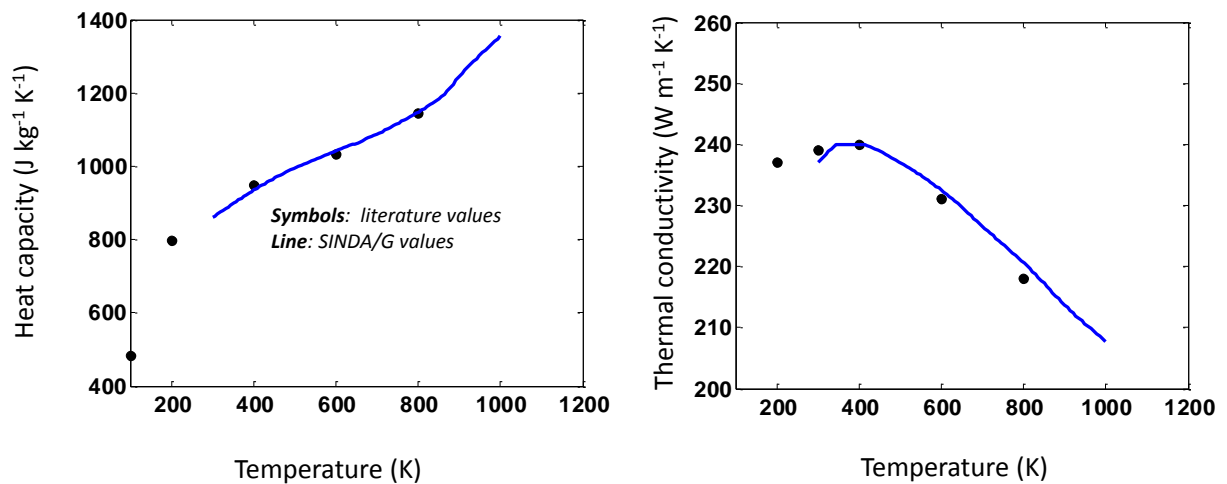
Appendix I – Thermal Properties

The thermal properties reported in this section are used for the reference model and considered base case values. Unless otherwise mentioned in the discussion, all analyses performed used the same thermal properties as the reference model.

Aluminum

Density=2702 kg m⁻³, Emissivity: 0.1

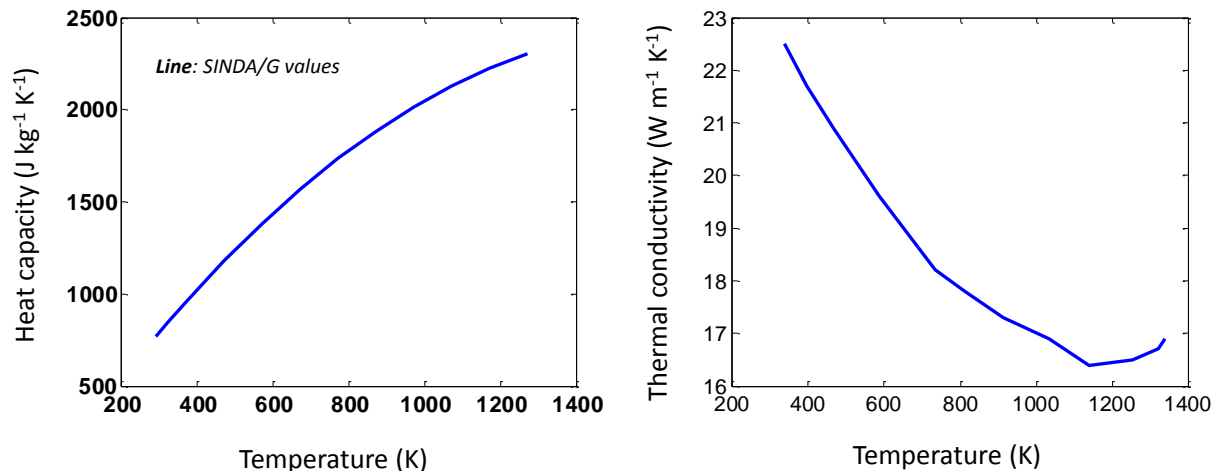
Properties are verified with literature values [8]. Emissivity is assumed constant and not a function of temperature. The properties used in SINDA/G code are also used for the Reference model.



Fuel

Density=1720 kg m⁻³, Emissivity: 0.8

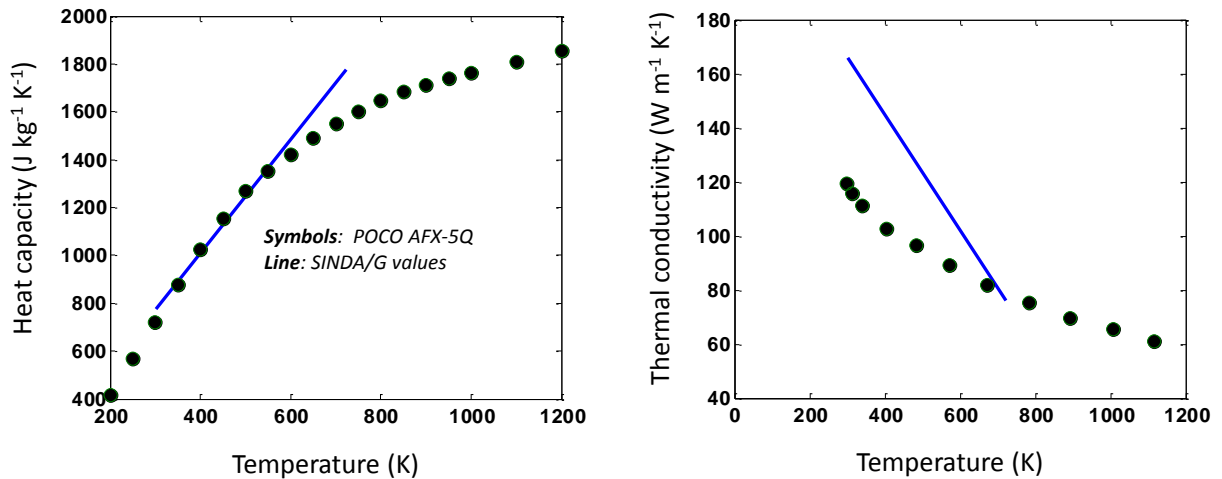
Properties are used in SINDA based on previous reported values for HEU fuel [2]. The properties used in SINDA/G code are also used for the Reference model.



Graphite

Density=1850 kg m⁻³, Emissivity: 0.8

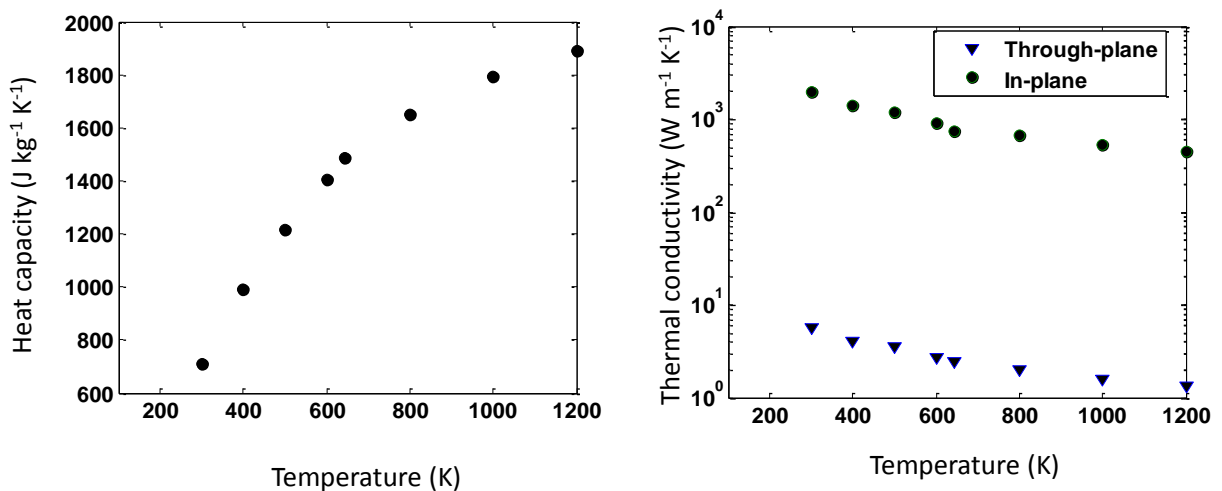
Properties are verified with commercial grade graphite [9]. Emissivity is assumed constant and not a function of temperature. Reference model uses conductivity and heat capacity values for *POCO AFX-5Q*.



Pyrolytic Graphite

Density=1850 kg m⁻³, Emissivity: 0.8

Properties reflect thermal pyrolytic graphite [6]. Emissivity assumed the same as for graphite.



Microporous insulation (Microsil®)

Density=230 kg m⁻³, Specific heat= 800 J kg⁻¹ K⁻¹

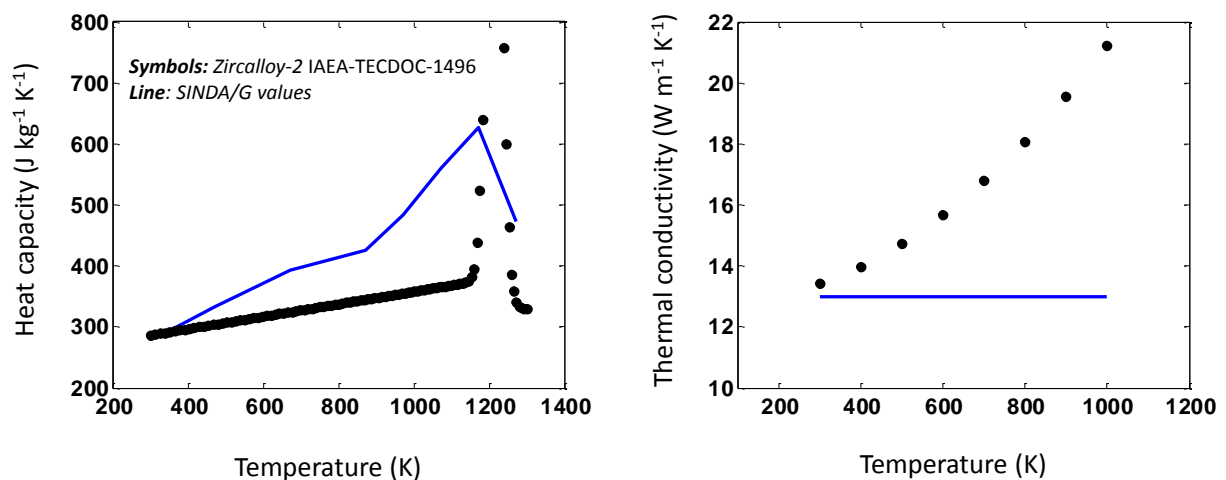
Thermal properties for Microsil® microporous insulation provided by Zircar ceramics was used as a reference material. Maximum service temperature is 950 °C. Higher temperature results in loss of mechanical strength properties. Thermal conductivity data are tabulated below.

Temperature (K)	Conductivity (W/m,K)
293	0.019
473	0.028
673	0.03
1073	0.038

Zircaloy

Density=6567 kg m⁻³, Emissivity: 0.3

Various data sources have been compared regarding the property values of Zircaloy [10-12]. Emissivity values of Zircaloy depend strongly on whether or not an oxide film is present. The value used in the calculation assumes an oxide free surface. The emissivity is to a good approximation independent of temperature. Recommended values for Zircaloy-2 [11] have been used in the reference model for heat capacity and thermal conductivity. Zircaloy-4 heat capacities may differ +/- 20% from Zircaloy-2.



Appendix II – Peak fuel and cladding temperatures for scoping analysis

The following table presents the peak fuel and peak cladding temperatures (corner region) for the reference and variant cases calculated. The reference case considers a 4 ft. long core, coolant air-flow (3250 cfm, 38 °C inlet temperature), 25 mil Zircaloy cladding separated by a nominal gap of 50 mil from the fuel. Calculations assume both thermal radiation and gas-phase heat conduction as heat transfer mode in the gap. A total core power history was used to produce a peak fuel temperature of 750 °C. Variants considered are: a) replacing fuel with pyrolytic graphite, b) effect of gap thickness, c) effect of convective heat transfer (HTFAC), and d) replacing part of the fuel with insulation.

Cases		Run#	Air flow (cfm)	Cladding (°C)	Fuel (°C)
Reference	50 mil gap	A1	3250	637	750
		A2	6500	564	750
		A3	8000	540	750
PyGr	Reference+60 mil PyGr	B1	3250	630	753
		B2	6500	556	753
	Reference+120 mil PyGr	B3	3250	618	753
		B4	6500	543	753
	Reference+180 mil PyGr	B5	3250	610	762
		B6	6500	534	765
	Reference+240 mil PyGr	B7	3250	604	776
		B8	6500	528	776
Air gap	110 mil gap	C1	3250	611	758
		C2	6500	520	758
	170 mil gap	C3	3250	610	772
		C4	6500	512	772
	230 mil gap	C5	3250	617	787
		C6	6500	512	787
Heat Transfer	(HTFAC = 1.75) ^{b)}	D1	3250	593	750
	(HTFAC = 5)	D2	3250	548	750
	(HTFAC = 10)	D3	3250	556	750
	(HTFAC = 2.85)	D4	3500	445	750
	(HTFAC = 5.71)	D5	6500	414	750
	(HTFAC = 8.57)	D6	6500	413	750
Table continued on next page					

Cases		Run#	Air flow (cfm)	Cladding (°C)	Fuel (°C)	T_{\max} cladding (min) ^{a)}
Insulation^{c)} (Micro-porous)	50 mil	E1	3250	455	755	6.6
		E2	6500	350	755	5.0
		E3	8000	319	755	4.6
	110 mil	E4	3250	331	770	9.8
		E5	6500	235	770	7.5
		E6	8000	211	770	6.9
	170 mil	E7	3250	268	776	12.6
		E8	6500	185	776	11.0
		E9	8000	166	776	10.0
Insulation (110 mil) (Effectiveness)	Micro-porous	E4	3250	331	770	9.8
	0.05 W/m,K	F1	3250	411	768	6.7
	0.08 W/m,K	F2	3250	491	768	5.7
	0.10 W/m,K	F3	3250	525	767	5.1
	0.12 W/m,K	F4	3250	552	767	4.6
	0.15 W/m,K	F4	3250	583	767	4.0
	110 mil gap	C1	3250	611	758	3.7
Insulation (170 mil) (Effectiveness)	Micro-porous	E7	3250	268	776	12.6
	0.05 W/m,K	G1	3250	346	775	9.3
	0.08 W/m,K	G2	3250	429	778	7.3
	0.10 W/m,K	G3	3250	467	778	6.5
	0.12 W/m,K	G4	3250	500	780	6.0
	0.15 W/m,K	G5	3250	532	778	5.3
	170 mil gap	C3	3250	610	772	4.0

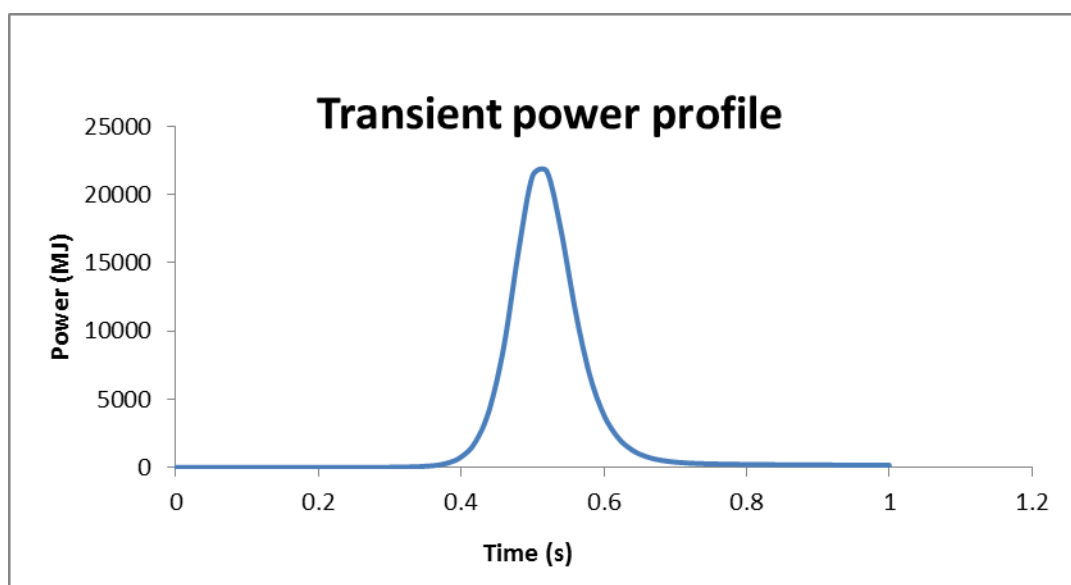
- a) T_{\max} cladding denotes the time when the cladding reaches its maximum temperature after the power pulse is initiated.
- b) Heat transfer coefficient increases by 1.75 as flow-rate doubles. A too high heat-transfer coefficient is not necessarily beneficial in reducing peak cladding temperatures. For all calculations in this report, it was assumed that the graphite reflector is in direct contact with the cladding. A high heat-transfer coefficient will also increase the temperature of the lower reflector (heat deposited from the gas-phase to the reflector) and minimize heat transfer by conduction/radiation from fuel to lower reflector.
- c) Thermal properties for Microsil® were used for microporous insulation, see Appendix I.

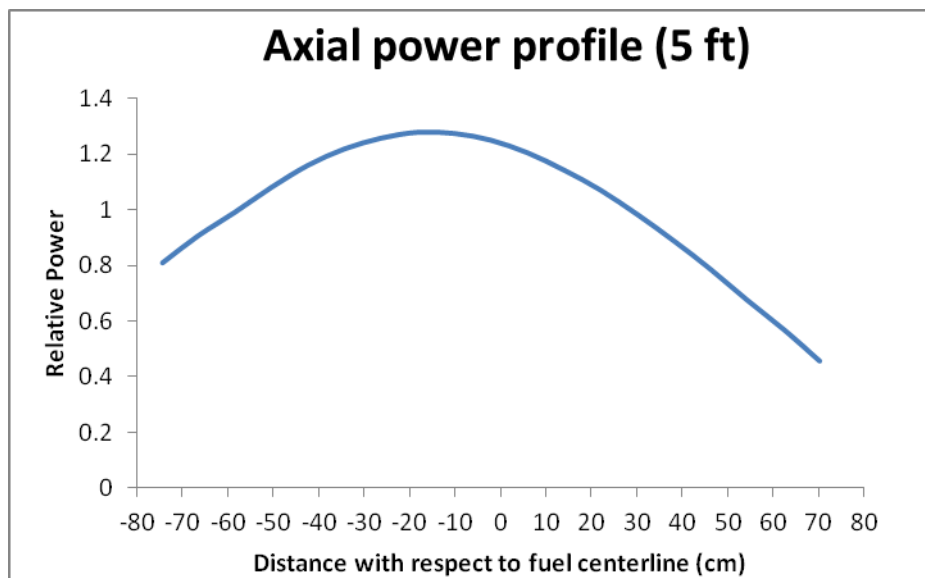
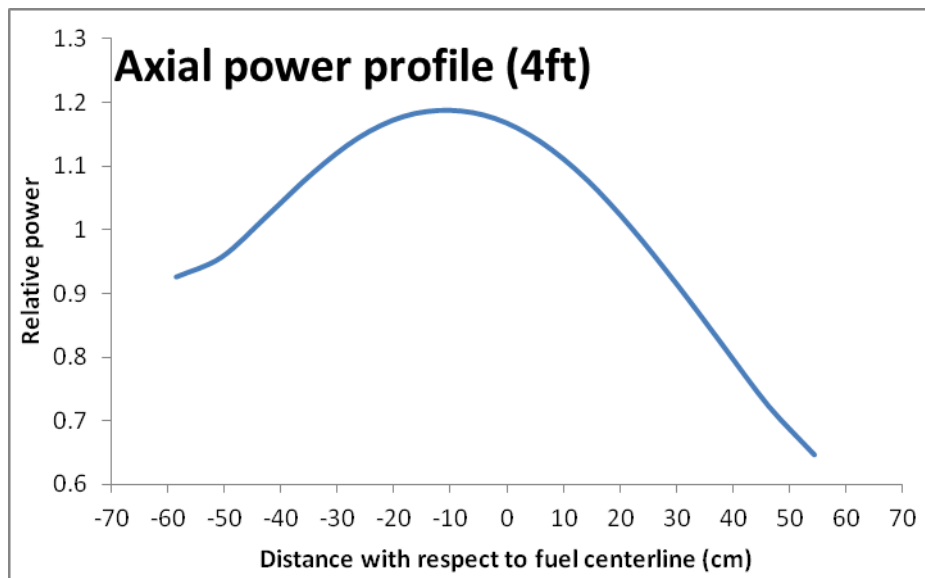
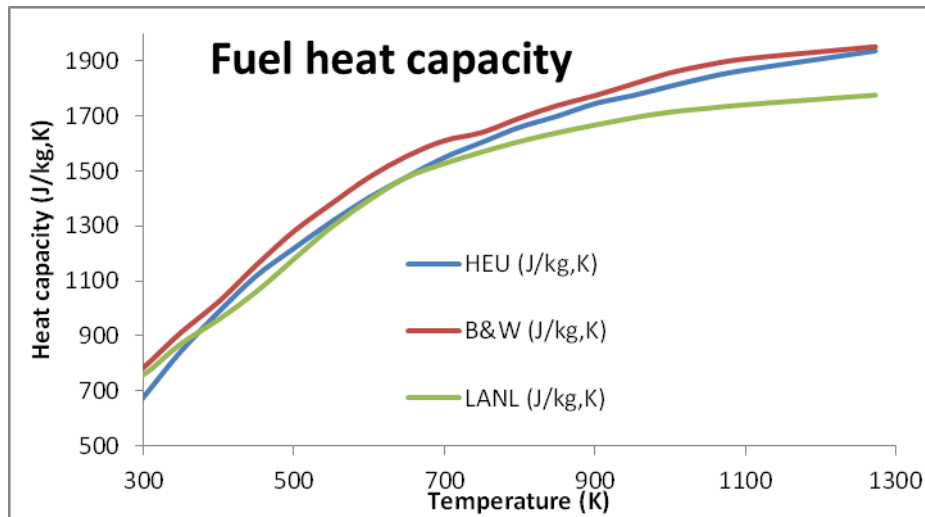
Appendix III - Supporting information for TREAT LEU design variants

Parameters used for the LEU base case and variants are reported below. The total core power and integrated energy (3 GJ) as calculated with TREKIN was used for comparison purposes. Power history and axial power profiles (as calculated with MCNP) for the hottest fuel assembly considered the case of 70% graphitization, 1.75g/cm³ fuel density, single Zircaloy cladding (including along the axial reflectors), and reflector in direct contact with the fuel column.

Parameter	Value/Assumptions	Unit/Comment
Coolant (air) inlet temperature	38	°C
Coolant flow rate	3000	CFM
Cladding (Zircaloy) thickness	25	mil (1/1000")
Cladding can length	8	ft.
Length of fuel section	4 or 5	ft.
Gap Fuel Column/Reflector	0	no gap
Cladding/Fuel meat nominal gap	50	mil (1/1000")
Ratio of fuel assembly power to total core power (4ft/5ft)	0.426/0.421	%
Total core energy (TH reference)	2970	MJ
Fuel density	1750	kg m ⁻³
Fuel heat capacity (low graphite content)	LANL	[7]
Fuel heat capacity (high graphite content)	B&W	[7]
Microporous insulation ^{a)}	Microsil®	www.zircar.com
Pyrolytic Graphite ^{a)} , density	2250	kg m ⁻³

Table 1. Parameters used for the LEU design variants. ^{a)} Properties reported in Appendix I





Appendix IV. Effect of vacuum quality on peak cladding temperature

A crucial issue in the TREAT fuel assembly design is what quality of vacuum would be needed to keep the cladding temperature below acceptable limits if conductive heat transfer within an evacuated gap is to be negligible. In the following calculations, the effect of pressure (vacuum quality) on thermal conductivity was estimated. The temperature of the cladding was then calculated for a range of pressures and correlated to the vacuum quality.

Given the high aspect ratio (length/thickness) of the gap in the fuel part of the assembly, the geometry is well approximated by parallel plates. As a good approximation, for parallel plates only, the relation originally developed by Kennard, 1938 was used to calculate the effect of pressure on the thermal conductivity [13,14]. The mean free path of air, CO, CH₄ as well as CO₂ is approximately in the same order. For simplicity, the gas in the gap was approximated by air. Figure 1 shows the reduced thermal conductivity as a function of pressure and gap distances. The reduced conductivity is expressed relative to that of air at 1 atm. For a gap distance of 50 mil, the conductivity is no longer independent of pressure at approximately 10 mbar. At ~ 0.1 mbar the mean free path of the gas equals the gap thickness and the conductivity decreases linearly as a function of pressure on a log-log scale. Reducing the conductivity by a factor of 1000 would necessitate that the pressure is approximately in the order of 10⁻⁴ mbar. Changing the temperature from 400 °C to 600 °C did not significantly affect the reduced thermal conductivity.

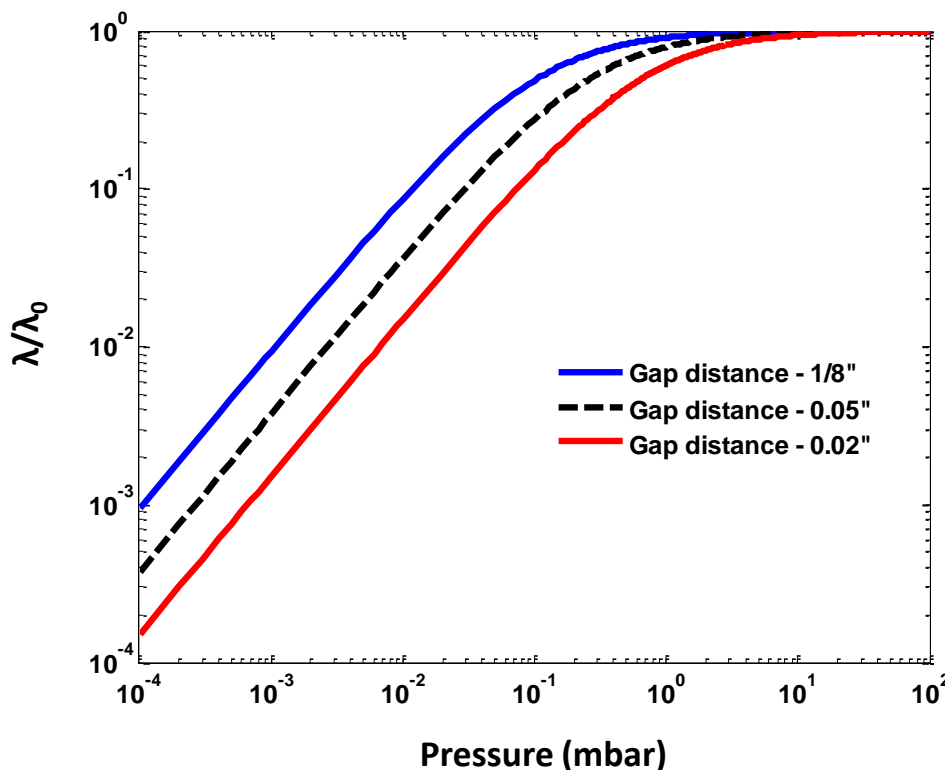


Figure 1. Relative reduction of the gas-phase conductivity as function of pressure

Calculations were done to delineate the peak-cladding wall temperature as an effect of thermal conductivity (assuming a gap distance of 50 mil). The case considered a 4 ft. fuel section and used the parameters, core power history and axial power profiles as given in Appendix III. The heat capacity for an HEU fuel was used resulting in a calculated peak fuel temperature of 615 °C.

Figure 2a (side wall) and 2b (far side, corner wall) show the peak cladding temperature as a function of reduced conductivity. The peak cladding temperature decreases steeply until the thermal conductivity is reduced by a factor of 10 relative to that at atmospheric pressure, and more gradually thereafter. As soon as the conductivity is reduced by a factor of 100 or more, the peak wall temperature remains constant and radiation heat transfer from fuel to cladding wall controls the heat transfer. As long as the reduced conductivity is less than 1/10, small changes in peak cladding temperatures are anticipated. According to Figure 1, this would translate to aim for a total pressure of approximately 0.05 mbar or less. The reduction in temperature from atmospheric conditions in the gas gap vs when radiation heat transfer controls heat transfer is more pronounced at the corner section (60 °C difference) vs ~22 °C as calculated in the side wall.

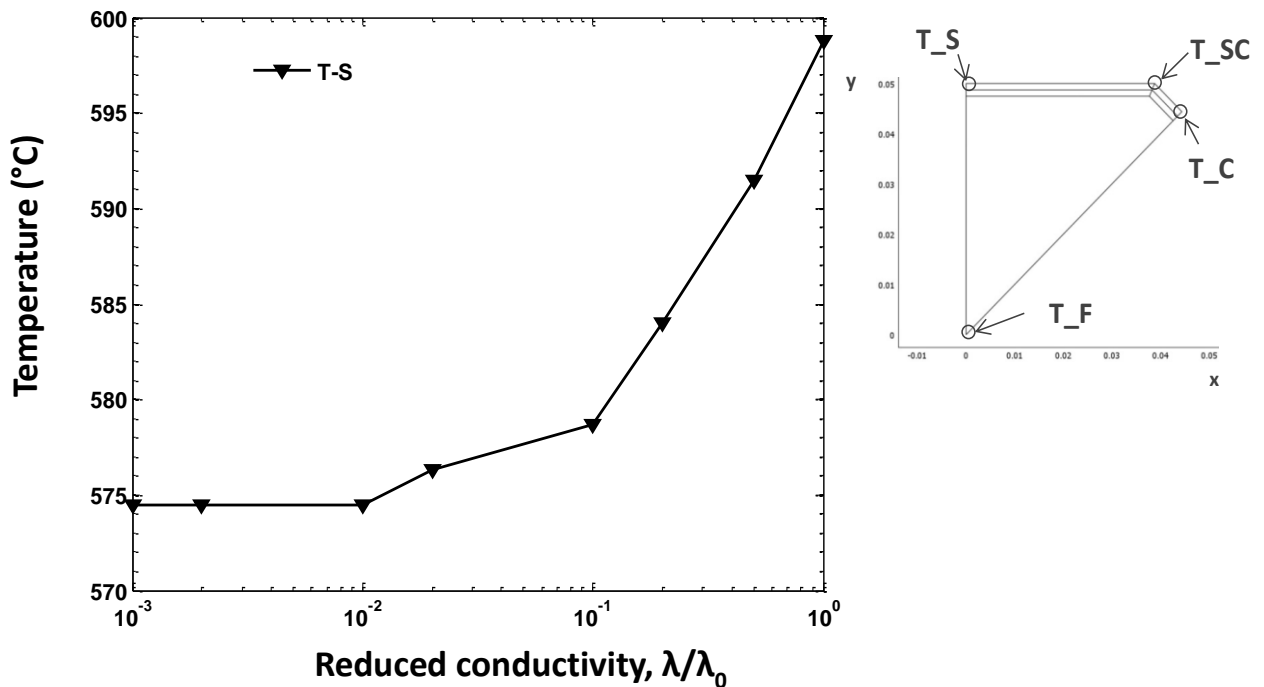


Figure 2a. Effect of gas-phase conductivity on the side wall (T-S) temperature.

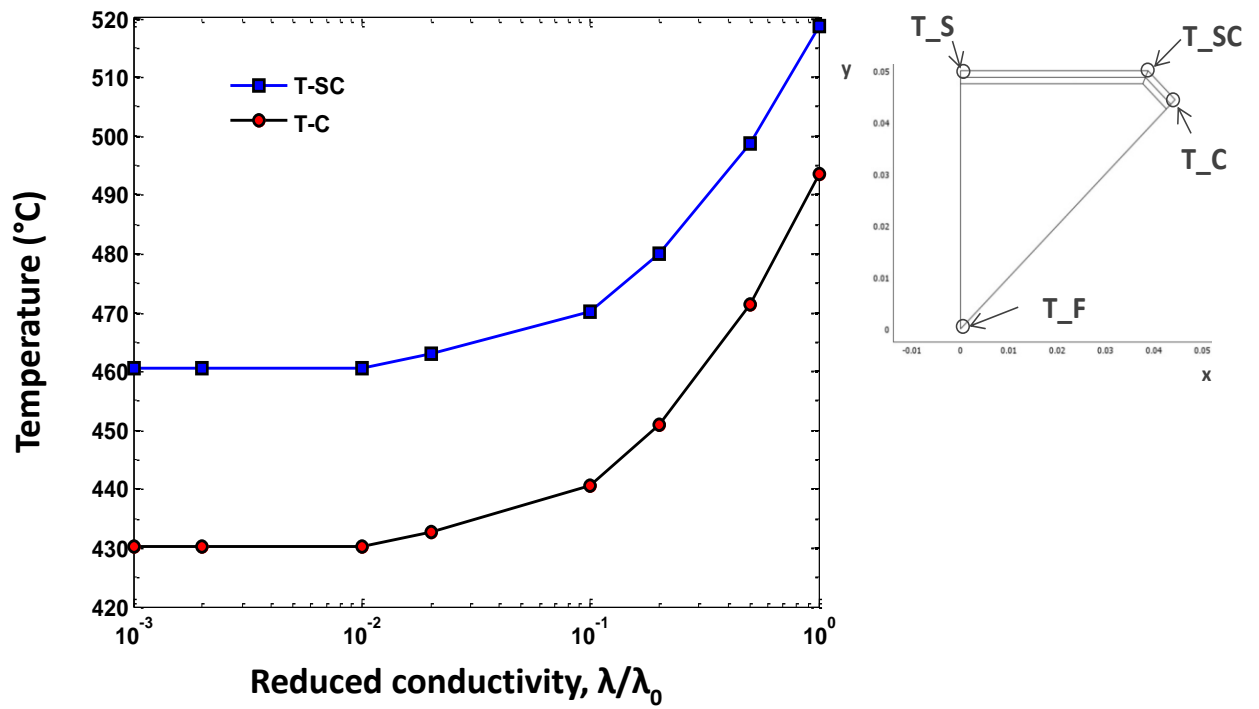


Figure 2b. Effect of gas-phase conductivity on the far side (T-SC) and corner wall (T-C) temperature.



Nuclear Engineering Division

Argonne National Laboratory
9700 South Cass Avenue, Bldg. 208
Argonne, IL 60439-4842

www.anl.gov



Argonne National Laboratory is a U.S. Department of Energy
laboratory managed by UChicago Argonne, LLC